Wubshet Belay Abagero

Exploring the potentialities of waste plant materials for the production of gold nanoparticles and multi-metallic composite particles and its application in wastewater treatment

UNIVERSIDADE DO ALGARVE
FACULDADE DE CIÊNCIAS E TECNOLOGIA
2017

Wubshet Belay Abagero

Exploring the potentialities of waste plant materials for the production of gold nanoparticles and multi-metallic composite particles and its application in wastewater treatment

Erasmus Mundus MSc in Chemical Innovation and Regulation
Mestrado Erasmus Mundus em Inovação Química e Regulamentação

Trabalho efetuado sob a orientação de:

Work supervised by:

Prof. Maria Clara Costa
Dr. Anahi Dandlen

UNIVERSIDADE DO ALGARVE
FACULDADE DE CIÊNCIAS E TECNOLOGIA
2017

Exploring the potentialities of waste plant materials for the production of gold nanoparticles and multi-metallic composite particles and its application in wastewater treatment

Declaration of Authorship

I declare that I am the author of this work, which is original. The work cites other authors and works, which are adequately referred in the text and are listed in the bibliography.

Wubshet Belay

Wubshet Belay Abagero

Exploring the potentialities of waste plant materials for the production of gold nanoparticles and multi-metallic composite particles and its application in wastewater treatment

UNIVERSIDADE DO ALGARVE
Faculdade de Ciências e Tecnologia
2017

Acknowledgment

First and foremost, I would like to express my gratitude to my supervisors; Prof. Maria Clara Costa and Dr. Anahi Dandlen for the continuous guidance, invaluable suggestions and encouragement throughout the study. Without their guidance at every stage, this thesis could never have been completed. I would also like to thank European Commission, the EMMC-ChIR management team, University of Algarve, University of Bologna, University of Barcelona, Heriot-watt University and CCMAR for giving me this great opportunity. I would like to express appreciation to Dr. Jorge Carlier, Tânia Luz Palma for the great help during my laboratory work. Last but for not least, I want to thank GOD for helping me to complete my thesis in due time.

Abstract

Biosynthesis of metallic nanoparticles has been regarded as a green, environmentally friendly and efficient method for nanoparticles production that avoids the usage of toxic chemicals and generation of hazardous waste during the process. In this study we reported a green, facile and rapid biosynthesis method for the synthesis of gold nanoparticles (AuNPs) and multi-metallic composite particles using raspberry leave extract as both reductant and capping agent in a single-pot process. Various waste plant materials were collected from the Algarve region for extract preparation. The waste plant materials were selected based on the availability and the cost of the material. Reduction potential of each extract was determined using FRAP method. Optimization of the synthesis method (synthesis time and metal precursor concentration) was investigated to get the best synthesis conditions. Standard gold-(III) chloride solution for AuNPs and AMD wastewater from São Domingos mine site, southwest Portugal, for multi-metallic composite particles was used as source of the corresponding metal ions. The UV–Vis spectra showed a SPR peak at 560nm for the AuNPs that were synthesized using optimized synthesis conditions which were 15 min synthesis time, 100 mg/L gold-(III) solution concentration and 1:10 (v/v) extract to standard gold (III) solution ratio at room temperature. TEM images of the precipitates obtained from Au-(III) solution showed different shape and sizes which consist of spherical NPs (51–70 nm), along with few rods (71–80 nm), triangular (61-70 nm) and hexagonal (61-70 nm) particles. TEM images of multi-metallic composite particles revealed there were mostly composed of spherical particles with an approximate average size of 100 nm (range between 70-150 nm). In XRD pattern, the crystalline natures of the synthesized AuNPs showed sharp intense peaks of Bragg reflections corresponding to (111), (200), (220), (311) and (222) planes at 2θ values of 38.2^0, 44.5^0, 64.7^0, 77.7^0 and 81.2^0, respectively, displays the crystalline nature of AuNPs and no other peaks were observed due to impurities. These planes are assigned to cubic structure of the AuNPs according to the high-Score Plus software with the ICDD PDF-2 database. The AuNPs were further characterized by Energy dispersive X-ray spectra (EDS) analysis, which gives additional evidence for the reduction of Au-(III) solution to elemental gold thus confirming gold as the only element in the precipitate. The EDS analysis for multi-metallic composite particles suggested that the particles are mainly composed by iron, aluminum and copper, probably as oxides. The stability of AuNPs and multi-metallic composite particles were measured using zeta potential and both particles showed moderate to good stability at different pH range and lower stability at pH 1 and pH 2. The application of the synthesized multi-metallic particles as adsorbent was tested for the removal of phosphate from synthetic wastewater and it showed up to 70.0 ± 3.9 % removal efficiency. In conclusion, in this study suitable, eco-friendly, nontoxic, and single pot synthesis method was developed for the production of AuNPs and multi-metallic composite particles using raspberry leave extract. This study also revealed the potential utilization of acid mine drainage wastewater as a source of multi-metallic composite particles which has proven efficiency to remove phosphate from wastewater via adsorption.

Contents

List of figures

List of abbreviation

NPs	Nanoparticles
AuNPs	Gold nanoparticles
AgNPs	Silver nanoparticles
FeNPs	Iron nanoparticles
TEM	Transmission electron microscopy
DLS	Dynamic light scattering (DLS)
UV-Vis	Ultraviolet-visible
ED	Electron diffraction
XRD	X-ray diffraction
EDS/EDX	Energy dispersive X-ray spectra
FRAP	Ferric Reducing Ability of Plasma
COD	Chemical Oxygen Demand
ANOVA	Analysis of variance
AMD	Acid Mine Drainage
FAAS	Flame atomic absorption spectroscopy
MP-AES	Microwave plasma-atomic emission spectroscopy
FAAS	Flame atomic absorption spectroscopy
SPR	Surface plasmon resonance
TPTZ	Tripyridyltriazine

1. Introduction

Nowadays nanoparticles and their technologies are booming rapidly due to their enormous applications namely water and wastewater treatment, pharmaceuticals, electronics, paints, cosmetics, catalysis, biosensor etc.). There is huge production of nanomaterial worldwide (Palaniselvam Kuppusamy M. M., 2016; C. Mystrioti, 2016). However the current manufacturing practice involves many chemicals which are toxic enough to pollute the environment and make the process unsafe during the large scale production of nanomaterial. Thus, exploring green synthesis methods, recovery of resource with less cost for the production of nanomaterials and their application is mandatory (C. Mystrioti, 2016). Hence, it is important to understand the following: what are the available resources, how can we recover resources from waste materials? How nanoparticles can be synthesized greenly without affecting its noble their properties? How can we optimize the application of nanomaterial in various areas such as wastewater treatment? (Palaniselvam Kuppusamy M. M., 2016; S.S. Godipurgea S. Y., 2016).

Nanomaterials are very important developing research area which has been an interest of most of researcher (María Martínez-Cabanas, 2016; P.P.N. Vijay Kumara, 2014; Jasmine Jacob, 2012; Palaniselvam Kuppusamy S. J., 2015). Due to the advantageous distinctive characteristics nanoparticles, their applications are growing promptly on various fields like water and wastewater treatment, biomedical, pharmaceutical, catalysis, drug delivery, antimicrobial, biosensor technology, Catalysts, conductors in various areas such as health sectors, food industry, manufacturing environmental, space industry, optical industries and so on (P. Mohanpuria, 2008; Amit Kumar Mittal, 2013; Niederberger, 2013). The change in the physico-chemical properties of nanoparticles is responsible for the mentioned novel functional attributes of nanoparticles (Niederberger, 2013; Shakeel Ahmed, 2016).

The main factors that nanotechnology depends on are the synthesis and modulation of nanoparticles, which significantly affect their properties. Because of the smaller particle size, various shapes and increased surface area, nanoparticles display very different properties than their bulk materials and are found to be interesting candidates for the numerous applications mentioned above (P.P.N. Vijay Kumara, 2014; P. Mohanpuria, 2008; Niederberger, 2013). Nanomaterials have been used unknowingly for thousands of years; for example, gold nanoparticles that were used to stain drinking glasses also cured certain diseases. Scientists have been progressively able to observe the shape and size dependent physiochemical properties of nanoparticles by using advanced techniques. Recently, the diverse applications of metal nanoparticles have been explored in biomedical, agricultural, environmental, and physiochemical areas (Niederberger, 2013).

Comparing to other nanoparticles, the metallic nanoparticles have been considered as the most promising as they contain remarkable properties due to their large surface area to volume ratio (Niederberger, 2013; Palaniselvam Kuppusamy M. M., 2016). Specific examples of gold nanoparticles applications include delivery of specific drug, such as paclitaxel, methotrexate, and doxorubicin. Gold nanoparticles have been also used for tumor detection, angiogenesis, genetic disease and genetic

disorder diagnosis, photo imaging, and photo thermal therapy (Khwaja Salahuddin Siddiqi, 2017). Silver nanoparticles have been used for many antimicrobial purposes, as well as in anticancer, anti-inflammatory, and wound treatment applications (J. Das, 2013; H. Joy Prabu, 2015; B. Ajithaa, 2016; Niederberger, 2013). Due to their biocompatible, nontoxic, self-cleansing, skin-compatible, antimicrobial, and dermatological behaviors, zinc and titanium nanoparticles have been used in biomedical, cosmetic, ultraviolet (UV)-blocking agents, and various cutting-edge processing applications (J. Das, 2013; B. Ajithaa, 2016; H. Joy Prabu, 2015; Niederberger, 2013).

Metallic nanoparticles are commonly used as adsorbent as in polishing steps to remove organic and inorganic contaminants in water and wastewater treatment. The efficiency of conventional adsorbents is usually limited by the surface area or active sites, the lack of selectivity, and the adsorption kinetics. Nano-adsorbents offer significant improvement with their extremely high specific surface area and associated sorption sites, short intraparticle diffusion distance, and tunable pore size and surface chemistry (H. Joy Prabu, 2015; Xiaolei Qu, 2013).

In addition, metallic nanoparticles have been used in the spatial analysis of various biomolecules, including several metabolites, peptides, nucleic acids, lipids, fatty acids, glycosphingolipids, and drug molecules, to visualize these molecules with higher sensitivity and spatial resolution (María Martínez-Cabanas, 2016; Niederberger, 2013; P. Mohanpuria, 2008). Moreover, the unique properties of metallic nanoparticles make them well suited for designing electrochemical sensors and biosensors. For example on its environmental applications, nano-sensors have been developed and used for the detection of algal toxins, mycobacteria, and mercury presence in drinking water. Nano-sensors are also applied for hormonal regulation and for detecting crop pests, viruses, soil nutrient levels, and stress factors. Moreover, nano-sensors for sensing auxin and oxygen distribution have been developed (H. Joy Prabu, 2015; B. Ajithaa, 2016; Khwaja Salahuddin Siddiqi, 2017; Michael Iv, 2015).

Recent investigations in nanotechnologies showed leapfrogging opportunities to develop next-generation water and wastewater treatment systems using nanomaterial (Akbar Soliemanzadeh, 2017; C.P. Devatha, 2016; Jing Liu, 2017). Our current water and wastewater treatment and discharge practices, which heavily rely on conveyance and centralized systems, are not always suitable and sustainable. The highly efficient, modular, and multifunctional processes enabled by nanomaterials are foreseen to provide high performance, affordable wastewater treatment solutions that less relies on large infrastructures. Nanomaterial based wastewater treatment promising not only to overcome the major challenges faced by existing treatment technologies, but also to provide new treatment capabilities that could allow reuse of treated wastewater (A. Jafaripour, 2015; D. Barrie Johnson, 2005; M.A. Martín-Lara, 2014).

Therefore, currently, there is an increasing demand to develop environmentally friendly and sustainable methods for the synthesis of nanomaterials that do not use toxic chemicals in the synthesis protocols so as to reduce the adverse impact on the environment and minimize health risks for human being. Various

metallic nanoparticles were successfully synthesized using different plant extracts (Arun Kumar Thalla, 2016; Palaniselvam Kuppusamy M. M., 2016). And also these nanoparticles tested for the application of industrial and domestic wastewater treatment and showed very promising pollutant removal efficiency. The green synthesis methods are advantageous over other conventional methods because they are simple, cost-effective, environmentally friendly, and easily scaled up for industrial scale synthesis (C. Mystrioti, 2016; Palaniselvam Kuppusamy M. M., 2016; Palaniselvam Kuppusamy M. M., 2016).

1.1 Nanoparticles: Synthesis methods

Over the last three decades the synthesis of nanoparticles has been drawn attention in the emerging areas of nanoscience and technology as particles in their nano form show different properties compared to the corresponding bulk material (P. Mohanpuria, 2008; Niederberger, 2013). Usually, metal nanoparticles can be synthesized through several chemical and physical methods. However, many chemicals used are toxic enough to pollute the environment during the large scale production of nanomaterial. Green synthesis methods have been adopted these days to reduce or eliminate the use or generation of toxic substances in the design, manufacture and applications of nanomaterial (H. Joy Prabu, 2015; J. Das, 2013; Khwaja Salahuddin Siddiqi, 2017; María Martínez-Cabanas, 2016; Muhammad Jamil Ahmed, 2015; P.P.N. Vijay Kumara, 2014; Amit Kumar Mittal, 2013; Peter Logeswari, 2015; Silvia Groiss, 2017).

Previous studies showed that various chemical have been explored for the synthesis of NPs (Amit Kumar Mittal, 2013; Jasmine Jacob, 2012; Niederberger, 2013; Shakeel Ahmed, 2016). Nowadays, Extracts of a diverse range of plant species have been successfully used in making NPs. In addition to plant extracts, microorganisms, plant tissue and fruits, plant and marine algae have been used to produce nanoparticles as alternative method to conventional chemical synthesis (Amit Kumar Mittal, 2013; Niederberger, 2013; P. Mohanpuria, 2008). Different types of nanomaterial such as silver, gold, iron, copper, zinc, titanium, magnesium and multi-metallic composite have been produced using this green alternative method. (Amit Kumar Mittal, 2013; Niederberger, 2013; P. Mohanpuria, 2008; Peter Logeswari, 2015). Among various metal nanoparticles, gold, silver, gold/silver composite, iron and multi-metallic composite particles nanoparticles are of particular interest and their green synthesis method still attracting scientists in the field of nanotechnology (Khwaja Salahuddin Siddiqi, 2017; Silvia Groiss, 2017; María Martínez-Cabanas, 2016; S.S. Godipurgea S. Y., 2016; C. Mystrioti, 2016).

Currently, there is an increasing demand to develop environmentally friendly and sustainable methods for the synthesis of nanomaterial that do not use toxic chemicals in the synthesis protocols. A number of approaches are available for the synthesis of nanoparticles, such as thermal decomposition, electrochemical, microwave assisted process and green synthesis. Many of the nanoparticle synthesis or production methods involve the use of hazardous chemicals, low material conversions and high energy requirements. This is the reason why there is a growing demand to develop environmentally friendly and safe processes for NPs synthesis (Khwaja Salahuddin Siddiqi, 2017; María Martínez-Cabanas, 2016; S.S. Godipurgea S. Y., 2016; Silvia Groiss, 2017; B. Ajithaa, 2016; Shakeel Ahmed, 2016; H. Joy Prabu, 2015).

Many studies showed that green synthesis methods are advantageous over other conventional methods because they are simple, cost-effective, environmentally friendly, easily scaled up for industrial scale synthesis (Ting Wang, 2014; C. Krishnaraj, 2010; B. Ajithaa, 2016; Jasmine Jacob, 2012; María Martínez-Cabanas, 2016; C. Mystrioti, 2016; C. Krishnaraj, 2010; Arun Kumar Thalla, 2016). In fact a number of bacteria, fungi, and yeast have been well known for the synthesis of nanoparticles (Niederberger, 2013; P. Mohanpuria, 2008). However, it is difficult, time consuming and expensive to use microbial mediated synthesis of nanoparticles industrially because it requires expensive medium (Amit Kumar Mittal, 2013; Niederberger, 2013). Therefore, the exploration of plant extracts as potential alternatives for the synthesis of nanoparticles has gained huge interest. Studies demonstrated that plants with high active ingredients such as water soluble antioxidant polyphenols, alkaloids, flavonoids etc, had reducing, capping or stabilizing ability to reduce metal into their respective nanoparticles (Amit Kumar Mittal, 2013; B. Ajithaa, 2016; Khwaja Salahuddin Siddiqi, 2017; M. Sigamoney, 2016; Muhammad Jamil Ahmed, 2015; María Martínez-Cabanas, 2016; C. Mystrioti, 2016; Arun Kumar Thalla, 2016) .

Generally nanoparticles can be produced in two ways, the first one is a “top down” approach and the second one is “bottom up” approach. In “top down” synthesis, nanoparticles are produced by size reduction from their respective suitable starting material. Size reduction can be achieved by various lithographic techniques *e.g.* grinding, milling, sputtering, thermal or laser ablation, etc. “Top down” method has disadvantage because it will not result perfect nanoparticles in terms of the surface structure and this is the main limitation of the process because the surface chemistry and the other physical properties of nanoparticles are highly dependent on the surface structure. In “bottom up” synthesis, the nanoparticles are built from smaller entities, for example by joining atoms, molecules and smaller particles. In this synthesis, the nanostructured building blocks of the nanoparticles are formed first and then assembled to produce the final particle. In this synthesis approach, nanoparticles can be produced using chemical (chemical reduction) or biological methods, such as the use of plants extract, micro-organisms, by self-assemble of atoms to new nuclei which grow into a particle of nanoscale (Amit Kumar Mittal, 2013; Khwaja Salahuddin Siddiqi, 2017; Niederberger, 2013; P. Mohanpuria, 2008).

In chemical synthesis of metallic NPs different organic and inorganic reducing agents, such as sodium borohydride (NaBH4), sodium citrate, ascorbate, elemental hydrogen, Tollen’s reagent, N, N-dimethyl formamide (DMF) and poly (ethylene glycol) block copolymers are used in aqueous or non-aqueous solutions as reducing agents. Capping agents are also used for size stabilization of the nanoparticles. One of the advantages of the chemical methods are a large quantity of nanoparticles can be synthesized in a short period of time. The main disadvantage of these syntheses methods are the fact that the chemicals in use might be toxic, making the production process unsafe and may have an impact on the environment (Shakeel Ahmed, 2016; Niederberger, 2013; P. Mohanpuria, 2008; C. Mystrioti, 2016). This is the reason why biosynthesis draw more attention of scientists in the area of nanoparticles production via green route that does not employ toxic chemicals and also doesn’t create any toxic waste (H. Joy Prabu, 2015; Khwaja Salahuddin Siddiqi, 2017; P.P.N. Vijay Kumara, 2014; Amit Kumar Mittal, 2013; M. Sigamoney, 2016; María Martínez-Cabanas, 2016; Arun Kumar Thalla, 2016). Thus, the advancement of

green syntheses of nanoparticles is progressing as a key branch of nanotechnology; where the use of biological entities like microorganisms and plants extracts for the production of nanoparticles could be an alternative to chemical and physical methods (Khwaja Salahuddin Siddiqi, 2017; Amit Kumar Mittal, 2013; Niederberger, 2013; P. Mohanpuria, 2008; S.S. Godipurgea S. Y., 2016). A summary of NPs synthesis method is described in the figure 1 below.

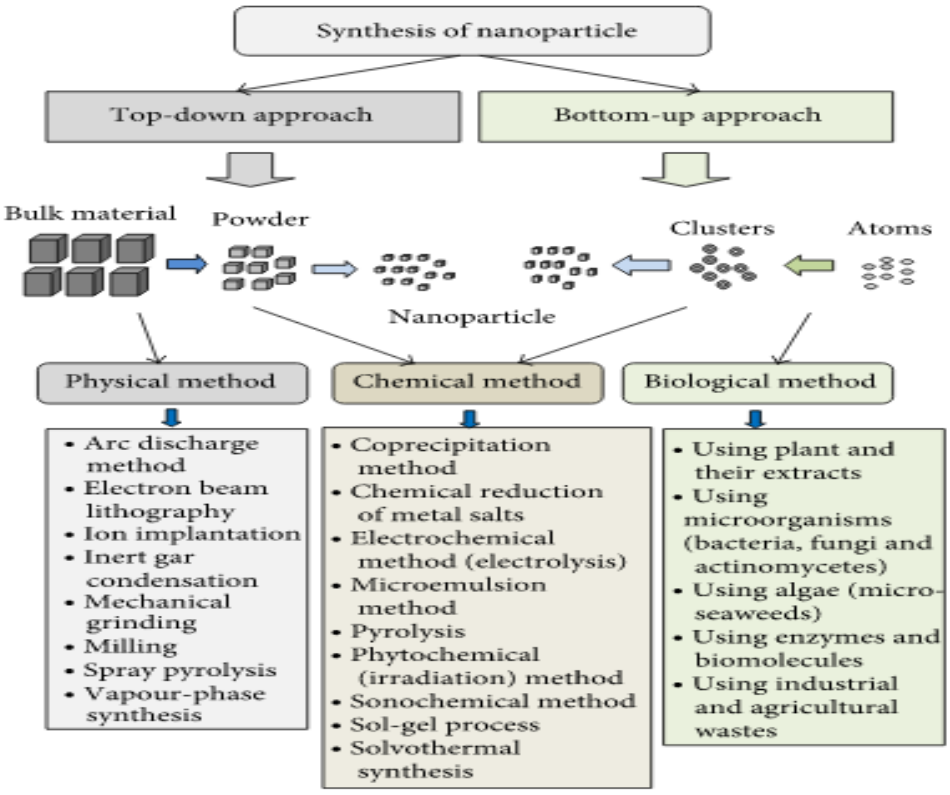

Figure 1 Summary of nanoparticles synthesis method *(Amit Kumar Mittal, 2013)*

Several methods have been developed for the biological synthesis of nanoparticles from salts of the corresponding metals as a safe and environmentally friendly alternative comparing to chemical synthetic procedures (Priyanka Singh, 2016; Amit Kumar Mittal, 2013; Muhammad Jamil Ahmed, 2015; Ting Wang, 2014; C. Mystrioti, 2016). Synthesis of nanoparticles using microorganisms or plants can possibly eliminate the problem mentioned. The use of plant extracts for the synthesis of nanoparticles could be advantageous over other environmentally friendly biological processes by eliminating the elaborate process of maintaining cell cultures. Biosynthesis methods are useful not only because of the reduced environmental impact and health hazard of the manufacturing process in comparison with some of the physicochemical production methods, but because they can be used to produce large quantities of nanoparticles that are free of contamination and have a well-defined size and morphology (Priyanka

Singh, 2016; Xiaolei Zhang, 2011; Khwaja Salahuddin Siddiqi, 2017; María Martínez-Cabanas, 2016; Muhammad Jamil Ahmed, 2015; Palaniselvam Kuppusamy S. J., 2015; Peter Logeswari, 2015).

1.2 Use of plant extracts in nanoparticle synthesis

Typically, a plant extract mediated reduction involves simply mixing the extract with an aqueous solution metal precursor at room temperature or at certain fixed temperature. Generally the synthesis complete within short time. Many researcher synthesized various nanoparticles of silver, gold, Iron and many other metals have been produced this way (Amit Kumar Mittal, 2013; B. Ajithaa, 2016; H. Joy Prabu, 2015; J. Das, 2013; Khwaja Salahuddin Siddiqi, 2017; M. Sigamoney, 2016; Muhammad Jamil Ahmed, 2015; Peter Logeswari, 2015; S.S. Godipurgea S. Y., 2016; C. Mystrioti, 2016). The nature of the plant extract, its concentration, the concentration of the metal salt, the pH, temperature, the addition of extract to the metal solution and contact time are known to affect the rate of production of the nanoparticles, their quantity and other characteristics (Jayachandra Reddy Nakkala, 2016; Amit Kumar Mittal, 2013; H. Joy Prabu, 2015; Peter Logeswari, 2015; Priyanka Singh, 2016; Khan Behlol Ayaz, 2014) .

Plant extracts may act both as reducing and stabilizing agent in the synthesis of nanoparticles (Amit Kumar Mittal, 2013). The source of the plant extract is known to influence the characteristics of the nanoparticles. This is because different extracts contain different concentrations and combinations of compounds such as phenolic, alkaloids, flavonoids etc. and the reduction process is relatively complex (Amit Kumar Mittal, 2013; H. Joy Prabu, 2015; Jasmine Jacob, 2012; María Martínez-Cabanas, 2016; Khwaja Salahuddin Siddiqi, 2017; C. Mystrioti, 2016).

Plant extracts are usually composed by different metabolites like terpenoids, phenols, proteins or carbohydrates. These compounds are directly responsible or the extract capacity to carry out the NPs biosynthesis. Each extract contains different concentrations and combination of reducing and stabilizing agents. Therefore, the extract composition determines the characteristics of synthesized NPs (Palaniselvam Kuppusamy M. M., 2016; Rani Mata, 2016; Jayanta Kumar Patra, 2016; Sathishkumar G., 2016; Amit Kumar Mittal, 2013; Akbar Soliemanzadeh, 2017). Comparing to other synthesis procedures, the use of plant extracts for making nanoparticles is simpler. Nowadays plant extract mediated synthesis of metallic NPs, such as AuNPs, AgNPs, FeNPs and multi-metallic composites, is attracting most of scientists' attention and explored a lot to get the best out of it (Arthanari Saravanakumar, 2015; Sathishkumar G., 2016; Amit Kumar Mittal, 2013; H. Joy Prabu, 2015; Jayachandra Reddy Nakkala, 2016; María Martínez-Cabanas, 2016; Palaniselvam Kuppusamy M. M., 2016). Processes for making nanoparticles using plant extracts are readily scalable, less expensive, and take shorter period of time in comparison with the relatively expensive and complex method of microbial synthesis (Amit Kumar Mittal, 2013; Priyanka Singh, 2016; Arthanari Saravanakumar, 2015; P. Mohanpuria, 2008; Khwaja Salahuddin Siddiqi, 2017; Arun Kumar Thalla, 2016).

In comparison to plant extract synthesis, the microbe mediated synthesis methods have several disadvantages such as high cost, need of identification of potential strain, maintenance of aseptic conditions for the profuse growth of microorganisms, chances of infection and contamination. Above all, the microbial synthesis methods are quite time consuming and require about 2-3 days for the growth of

a suitable strain and another 1-2 days for the synthesis and purification of NPs. As a result, scientists switched over their interest toward plant extract synthesis methods (Priyanka Singh, 2016; P. Mohanpuria, 2008; Palaniselvam Kuppusamy M. M., 2016; Xiaolei Zhang, 2011; Utkarsha Shedbalkar, 2014).

Table 1 Summary of previous studies on plant mediated synthesis of nanoparticles and their applications.

Plants and parts of the plant used	**Nanoparticles produced**	**Size and shape**	**Application**	**Reference**
Grape marc Black tea Vine leaves	Fe	15-45 nm, -	Degradation of ibuprofen	(S. Machado, 2013)
Camellia sinensis leave *Syzygium aromaticum* leave *Mentha spicata* leave *Punica granatum* juice Red Wine juice	Fe	60 nm, -	Cr(VI) reduction	(C. Mystrioti, Comparative evaluation of five plant extracts and juices for nanoiron synthesis and application for hexavalent chromium reduction, 2016)
Mangifera indica leave *Murraya Koenigii* leave *Azadiracta indica* leave	Fe	50-150 nm, Spherical	Treating domestic waste water	(Arun Kumar Thalla, 2016)
Green Tea	Fe	20-50 nm Circular	Degradation of concentrated dye mixtures	(Adam Truskewycza, 2016)
Eucalyptus leaf	Fe	160 nm Irregular spherical	Removal of phosphate	(Dan Cao, 2016)
Cynometra ramiflora	FeO	- Spherical	Antibacterial and Catalytic effect	(Silvia Groiss, 2017)
Eucalyptus leaves	FeO	-	As(V) removal	(María Martínez-Cabanas, 2016)
Green tea *Eucalyptus leaves*	Fe	Spheroidal	Removal of nitrate in aqueous solution	(Ting Wang, 2014)
Green tea leave	Fe	40-80 nm, -	Removal of Cr(VI)	(Akbar Soliemanzadeh, The application of green tea extract to prepare

				bentonite-supported nanoscale zero-valent iron and its performance on removal of Cr(VI): Effect of relative parameters and soil experiments, 2017)
Green tea Oolong tea Black tea	Fe	40-50 nm, Spherical	Degradation of malachite green	(Lanlan Huang, 2014)
Onion peel	Au	25-70 nm, Spherical Triangular	Antibacterial Antioxidant	(Jayanta Kumar Patra, 2016)
Piper *longum fruit*	Au	56 nm Spherical	Antioxidant Catalytic activities	(Jayachandra Reddy Nakkala, 2016)
Salicornia brachiate	Au	25-35 nm face centered cubic	Antibacterial Catalytic activities	(Khan Behlol Ayaz, 2014)
Plumeria alba flower	Au	15 and 28 nm, Spherical	Catalytic degradation of organic dyes and inhibit bacterial growth	(Rani Mata, 2016)
Couroupita guianensis fruit	Au	25 nm, Spherical Triangular Hexagonal Face centered cubic	Antioxidant activity	(Sathishkumar, 2016)
Capsicum annuum var. grossum pulp	Au	6-37 nm Triangle Hexagonal Quasi- spherical	Catalytic activity	(Chun-Gang Yuan, 2017)
Pogestemon benghalensis (B) O. Ktz. leaf	Au	10-50 nm Spherical Triangular	Photocatalytic activity degradation of methylene blue	(Bappi Paul, 2015)
Moringa oleifera flower	Au	3-5 nm Spherical	anti-cancer and catalytic activity	(K. Anand, 2015)

		Hexagonal Triangular		
Green and red cabbages	Ag, Au and bimetallic (Ag/Au)	20nm (Au) Triangular(Au) Spherical(Au) Spherical (Au/Ag) 25nm (Au/Ag)	-	(Jasmine Jacob, 2012)
Aerial parts of *R. hypocrateriformis*	Ag, Au and Au-Ag alloy	10-50 nm, Spherical	Antimicrobial Antioxidant Anticancer activities	(S.S. Godipurgea S. Y., 2016)
Cassia tora leave	Ag	- Spherical Hexagonal Irregular	Antioxidant Antibacterial activities	(Arthanari Saravanakumar, 2015)
Sesbania grandiflora leave	Ag	16 nm, Spherical cubic	Antimicrobial activity	(B. Ajithaa, 2016)
Acalypha indica leaf	Ag	20-30nm cubic face-centered	antibacterial activity against water borne pathogens	(C. Krishnaraj, 2010)
Tragia involucrate leave *Cymbopogon citronella Solanum verbascifolium* leave *Tylophora ovata* leave	Ag	40-45 nm Spherical face-centered cubic	-	(H. Joy Prabu, 2015)
Sesbania grandiflora leave	Ag	10-25, Spherical	Antibacterial human pathogens	(J. Das, 2013)
Onion extracts	Ag	5-10 nm Spherical	preparation of a modified electrode for determination of ascorbic acid	(Mohammad A. Khalilzadeh, 2016)
Skimmia laureola leave	Ag	38 nm Spherical Hexagonal	Antibacterial activity to human pathogens	(Muhammad Jamil Ahmed, 2015)
Ocimum tenuiflorum leave *Solanum tricobatum*	Ag	22-65 nm Irregular shape	antimicrobial activity against pathogenic	(Peter Logeswari, 2015)

leave	bacteria
Syzygium cumini leave	
Centella asiatica leave	
Citrus sinensis peel	

1.3 Use of plant extracts for treatment and for metal recovery from metal bearing wastewaters

Anthropogenic sources are the main responsible for the generation of Metals bearing wastewaters, which cause huge environmental and health impacts. In particular, various industries are, to a large extent, responsible for the pollution of the environment worldwide (M.A. Martín-Lara, 2014; Moo Joon Shim, 2015; K. Vijayaraghavan a, 2015). Several studies have shown that a large number of active and abandoned mines sites are significant contributors to heavy metal pollution of water bodies and soils (Evgenia Iakovleva, 2015; Young-Soo Han, 2017). This deterioration of environmental conditions is the major contributory factor that hinders sustainable development. Conventional methods such as chemical precipitation, ion exchange and other processes have a number of shortcomings; which are production of large secondary solid waste, high capital, chemical and operating costs (E.Y. Seo, 2017; A. Jafaripour, 2015; Evgenia Iakovleva, 2015; M. Kobya, 2017).

Therefore, there is a need to investigate new and sustainable ways of treating and recovery of metals from metal bearing wastewaters. Reduction of metals from metal-bearing wastewaters using plant extracts and application of the recovered metal particles as adsorbents for other wastewaters treatment can be sustainable in terms of avoiding environmental pollution and resource recovery (Olivier Lefebvrea, 2012; D. Barrie Johnson, 2005; K. Vijayaraghavan a, 2015).

1.4 Characterization of nanoparticles

The characterization of nanoparticles is an essential step in biosynthesis of nanoparticles. The shape, size, morphology, surface area, stability, and their dispersion are some of the properties used to characterize the synthesized nanoparticles. Homogeneity of these properties is important in many applications. The common techniques which are used by most of investigators for characterizing nanoparticles and to control synthesis processes are: Ultraviolet–visible (UV-Vis) spectrophotometry, Dynamic light scattering (DLS), Scanning electron microscopy (SEM), Transmission electron microscopy (TEM), Fourier transform infrared spectroscopy (FTIR), Powder X-ray diffraction (XRD) and Energy dispersive spectroscopy (EDS) (Adam Truskewycza, 2016; Amit Kumar Mittal, 2013; Chun-Gang Yuan, 2017; Chun-Gang Yuan, 2017; Jayanta Kumar Patra, 2016; K. Anand, 2015; Mohammad A. Khalilzadeh, 2016; Silvia Groiss, 2017). Common methods for characterization of nanoparticles are discussed in the table 2 below.

Table 2 Common methods for characterization of nanoparticles.

Characteristics	Characterization Techniques	Applications	References
Size and morphology of nanoparticles	Transmission electron microscopy	Most commonly used the technique for determination of the size, shape and morphology of the nanoparticles. Capable of displaying magnified images of a thin specimen, typically with a magnification in the range 10^3 to 10^6, higher resolution compared with the scanning electron microscopy.	(Sovan Lal Pal, 2011; Egerton, 2005; Amit Kumar Mittal, 2013)
	High-resolution transmission electron microscopy	Determine the arrangement of the atoms and their local microstructures, such as lattice fringe, glide plane, lattice vacancies and defects, screw axes, and surface atomic arrangement of crystalline nanoparticles	(Amit Kumar Mittal, 2013; C. Krishnaraj, 2010; Egerton, 2005)
	Scanning electron microscopy	Determine the morphology by direct visualization. This method is based on electron microscopy and offers several advantages for morphological and size analysis; however, it is also associated with several disadvantages, such as the ability to provide only limited information about the size distribution and true population average.	(Egerton, 2005; H. Joy Prabu, 2015; P.P.N. Vijay Kumara, 2014; Peter Logeswari, 2015; Sovan Lal Pal, 2011)
	Atomic force microscopy	Determine the size information (length, width, and height) and other physical properties (such as morphology and surface texture)	(Sovan Lal Pal, 2011; Amit Kumar Mittal, 2013; K.D. Lee, 2015)
	Dynamic light scattering	Dynamic light scattering (DLS) can also be used to characterize the surface charge and the size distribution of the particles	(Amit Kumar Mittal, 2013; Masumeh Noruzia, 2011; Pooriya Khademi-Azandehi, 2015)

		suspended in a liquid. This technique is also used by many scientists for the characterization of nanoparticles.	
Formation of nanoparticle	Ultraviolet-visible spectrophotometry	It is used to confirm the formation of nanoparticles by measuring Plasmon resonance and evaluating the collective oscillations of conduction band electrons in response to electromagnetic waves. That provide information regarding the size, structure, stabilization, and aggregation of nanoparticles	(Arthanari Saravanakumar, 2015; Bappi Paul, 2015; C. Mystrioti, 2016; Chun-Gang Yuan, 2017; Jayanta Kumar Patra, 2016; S.S. Godipurgea S. Y., 2016; Arun Kumar Thalla, 2016)
Crystallinity	X-ray diffraction	Powerful nondestructive technique. It provides information on crystal structure, phase, preferred crystal orientation (texture), and other structural parameters, such as average grain size, crystallinity, strain, and crystal defects.	(Sovan Lal Pal, 2011; C. Suryanarayana, 1998; C. Krishnaraj, 2010; Khan Behlol Ayaz, 2014)
Surface charge	Zeta potential	Determine the stability and surface charge of the colloidal nanoparticles, as well as the nature of the materials encapsulated inside the nanoparticle or coated on its surface	(Pooriya Khademi-Azandehi, 2015)
	Fourier transform infrared spectroscopy	Used to identify organic functional groups attached to the surface of nanoparticles and the surface chemistry of biogenic nanoparticles	(Amit Kumar Mittal, 2013; Shakeel Ahmed, 2016; Arun Kumar Thalla, 2016)
Other techniques	Energy dispersive X-ray spectra (EDS)	Identification of the elemental composition of the nanoparticles	(J. Das, 2013; Jayachandra Reddy Nakkala, 2016; Jayanta Kumar Patra, 2016)

1.6 Factors influencing the synthesis of metallic nanoparticles using plant extract

The properties of the synthesized nanoparticle depend on the pH of the synthesis medium, temperature, time, concentration of plant extract and the metal salt (Palaniselvam Kuppusamy M. M., 2016). All of these conditions are discussed below.

1.6.1 pH

pH is an important factor that influences the synthesis of nanoparticles by green methods. A study by reported the variation in pH of a solution is responsible the different size and shapes of nanoparticles formation (Shankar S.S., 2003). Another study has discovered that pH of the medium influences the size and texture of the synthesized nanoparticle which proved nanoparticle size can be controlled by varying the pH of the solution media (V. Armendariz, 2004).

1.6.2 Time

The synthesis time (the reduction time) is another factor that affects the characteristics of nanoparticles. The optimum reduction time produces high absorbance and sharp peak value that indicates higher concentration nanoparticles in the medium. This determines the characteristics of the synthesized NPs namely their size and shape that can be spherical, triangular, hexagonal and rectangular. In studies in which the synthesis of NPs finished within the short period of time the SPR (Surface plasmon resonance) peak get broader as the time goes on, which indicates size and yield increment. The size variations as a function of time may be due to several factors such as aggregation of particles (Bappi Paul, 2015; Chun-Gang Yuan, 2017; Jia Yu, 2016; Jayachandra Reddy Nakkala, 2016).

1.6.3 Temperature

Temperature is also another important factor that affects the synthesis of nanoparticles. In comparison to other synthesis methods, green synthesis requires minimum temperatures or even room temperature is generally enough. A study showed that the temperature of the reaction medium determines the nature of the nanoparticle formed (A. Rai, 2006). Another study also revealed the effect of temperature on the synthesis of nanoparticles. It showed that at high temperatures, it lead to the formation of higher spherical nanoparticles and triangular nanoparticles, whereas at lower temperature mostly increased triangular NPs formation increased (Raju, 2011). Another study reported different UV-Vis spectrophotometer absorbance spectra of gold nanoparticles and silver nanoparticles were obtained at different temperature. The peak sharpness increases with an increase in the reaction temperature. Most likely this might occurred due to an increase in the reduction rate at higher temperatures (Amarendra Dhar Dwivedi, 2010).

1.6.4 Concentration of metal ion or metal salt

The concentration of metal precursors could change the size of the synthesized nanoparticles. Increasing trend of particle size was observed with increasing concentration of metal ion in solution from 0.1 to 5.0 mM (Shashi Prabha Dubeya, 2010). TEM and UV-Visible result revealed that as the concentration of silver nitrate and auric acid increase, larger sized silver and gold nanoparticles were synthesized (Shashi Prabha Dubeya, 2010). A Similar trend was shown in another study: An increase in the concentration of the metal ion from 0.1–5 mM ratio, result in an increase in the particle size observed at the end of the synthesis (30 minutes) (Amarendra Dhar Dwivedi, 2010). In another study, the absorption increased steadily as the Au (III) concentration increased in the reaction mixture from 1 mM to 5 mM. It was

concluded that an increase in the concentration of available ions in a solution increases the yield of nanoparticles. While increasing the substrate concentration the large size and aggregation of nanoparticles was occurred due to the occurrence of competition between gold ions and functional groups (Nabeel Ahmad, 2017).

1.6.5 Metal precursors to extract volume ratio

The volume ratio of the solution of metal precursor and extract has an effect on the characteristics of nanoparticles produced. On a study done on the production of iron nanoparticles, the polyphenols extract was mixed with an iron (III) solution at certain volume ratios (i.e. 1:2, 1:1, 2:1). The maximum concentration of iron particles in suspensions was observed at a mixing ratio of iron (III) solution to extract (v/v) equal to 2 (C. Mystrioti, 2016). Another study was conducted with different leaf extract concentration ratio, (v/v) varied from 1:30, 2:30 and 3:30 of silver nitrate and auric acid solutions for the synthesis of silver and gold nanoparticles. As the ratio increased in favor of leaf extract, UV-vis spectra sharpness increased which was correlated with the formation of more nanoparticles (Amarendra Dhar Dwivedi, 2010). A report on a green synthesis of AuNPs revealed the increase of the intensity of the band of AuNPs as a consequence of an increase volume of leaf extract. The peak starts becoming narrower and narrower with further increase in volume of leaf extract, which indicated more nanoparticles formation but no size increment (Nabeel Ahmad, 2017).

1.6.6 The surrounding environment

The surrounding environment where the nanoparticles produced also contributes a lot in determining the characteristics of the synthesized nanoparticles. In various environmental conditions, nanoparticle might become core-shell nanoparticles quickly by absorbing materials or reacting with other materials from the environment through the process of oxidation or corrosion (V. Sarathy, 2008). To mention an example that showed the effect of the environment on the nature of the synthesized nanoparticles, the crystalline nature of the zinc sulphide nanoparticles changed immediately when its environment was changed from a wet to a dry condition (S. V. N. T. Kuchibhatla, 2012).

1.7 Application of NPs in wastewater treatment

Nowadays greenly synthesized nanoparticles are being used in cost effective and ecofriendly water treatment techniques attracting many scientists in the field wastewater. Thus, various NPs have been used for the treatment of different kind of wastewaters with specific characteristics. Iron and iron oxide NPs has been successfully used since very promising results have been reported by many investigators for the removal/degradation of various pollutant from water/wastewater: Degradation of ibuprofen (S. Machado, 2013), Cr (VI) reduction (Akbar Soliemanzadeh, 2017),treating domestic wastewater (C.P. Devatha, 2016), removal of phosphates (Dan Cao, 2016), As(V) removal (María Martínez-Cabanas, 2016), removal of nitrate from aqueous solution (Ting Wang, 2014), degradation of malachite green (Lanlan Huang, 2014) are several examples in which NPs were used.

As it is mentioned above, the best characteristic of nanoparticles comes from its small size that provides them their distinctive properties. However, their size makes difficult their use in certain applications such as water treatment due to the extremely complex separation of the material from solution. The immobilization of the synthesized materials onto porous solids is a good procedure to avoid this operational problem and to allow their reuse in several sorption cycles (C.K.S. Pillai, 2009). In addition, the immobilization helps to enhance certain properties of the materials such as their stability and mechanical strength. However, the immobilization process may also imply some disadvantages such as the reduction of NPs sorption capacity by blocking their binding sites or the deceleration of sorption kinetics. The choice of the immobilization matrix determines the physical and chemical properties of the final material; therefore the selection of an appropriate matrix is an important step to develop an adequate sorption procedure. Several compounds such as chitosan, alginate, silica, polyacrylamide or polyvinyl alcohol have been used as immobilization matrixes. (María Martínez-Cabanas, 2016; C.K.S. Pillai, 2009).

1.7.1 Phosphate removal from wastewater

Phosphorus (P) is an essential macroelement for plant and algae growth; however its disproportionate presence as phosphate in aquatic ecosystems can lead to deterioration of water quality. Phosphate is a limiting nutrient in the environment and it is one of the pollutants that cause eutrophication of water bodies. High amounts of phosphate can cause algal blooms and depletion of dissolved oxygen in the water bodies with negative impacts on the aquatic organisms. Human activities such as animal manure and fertilizer application in soil or discharge of industrial, domestic and agricultural wastewater are responsible for the enrichment of surface water with phosphate loadings (Dimitris Mitrogiannis, 2017). To make the problem worse, there are few removal mechanisms under normal operating conditions of wastewater treatment plants. Thus a system must be amended specifically with compounds to bond to or adsorb phosphate (Hossain M. Azam, 2014).

There are various physical, chemical and biological methods that have been proposed for phosphate removal from water or wastewater such as anion exchange, sorption, chemical precipitation, membrane nanofiltration, reverse osmosis, electrodialysis and biological removal through constructed wetland, activated sludge and microalgal systems (Dimitris Mitrogiannis, 2017). However, nowadays the most widely used methods are biological removal and chemical precipitation. Yet, these methods have limitations such as lower removal efficiency, high cost, undesired waste sludge production, pH dependence, temperature dependence, effect the organic load regarding on biological removal (BOD:N:P ratio), and requirement of large space. In addition chemical precipitation requires high input of chemical reagents and also the management of the sludge produced. On the other hand, adsorption by using metallic particles is considered as an efficient, simple and low-cost method for PO_4^{-3}-P removal even at low phosphate concentrations (Hossain M. Azam, 2014; Pei Luo, 2017; Asya Drenkova-Tuhtan, 2017).
Earlier studies have shown promising phosphate removal via adsorption using: zero valent iron (ZVI) (Nathalie Sleiman, 2017), ZnFeZr adsorbent (Asya Drenkova-Tuhtan, 2017), nanosized lanthanum hydrous doped on magnetic graphene nanocomposite (Hamid Rashidi Nodeh, 2017) and iron oxide

nanotubes (Minseok Kim, 2016). Therefore, it is important to find efficient alternative adsorbents with affordable price and sustainable production to protect the environment from phosphate pollution.

1.7.2 Factors affecting phosphate removal via adsorption

There are different factors that affect phosphate removal efficiency via adsorption. These are adsorbent particle size, pH of the wastewater, temperature, adsorbent-wastewater (m/v) ratio, which is related to the adsorption capacity, kinetics and separation of the adsorbent from the liquid phase (Dimitris Mitrogiannis, 2017).

1.8 Objective of the study

The main objective of this work was to explore the reduction potential of various waste plant materials for the synthesis of gold nanoparticles and the treatment of acid mine drainage wastewater via removal of metals aiming additional production of multi-metallic composite particles as well as their application as phosphate adsorbents from synthetic wastewater. The following are the specific objectives of the study.

- ✓ Identification of the potential of extract of waste plant materials for the synthesis of gold nanoparticles and multi-metallic composite particles.
- ✓ Green synthesis of gold nanoparticles using selected extract of waste plant material
- ✓ Removal of metals from acid mine drainage wastewater aiming the production of multi-metallic composite particles.
- ✓ Assess the potential application of the multi-metallic composite particles obtained from acid mine drainage as phosphate adsorbent, aiming phosphate removal from wastewaters.

Generally, this study intends to hit three birds with one stone. First, it will explore the potential of waste plant materials for the synthesis of gold nanoparticles and for the production of a multi-metallic composite particles from acid mine drainage, thus turning wastes into useful materials. Second, it aims to apply the composite obtained to other wastewater treatment. Third, it will reduce the operational, chemical and sludge management cost required by other traditional wastewater treatment systems.

2. Experimental Part

2.1 Chemicals and Materials

The following chemicals were used in the present work:
Standard gold (III) chloride solution (Sigma-Aldrich, gold atomic spectroscopy standard concentrate, 1.00 g/L Au standard solution) was used to pre, anhydrous ethanol (96% vol, VWR International Laboratory Chemicals) was used in the extraction process. To conduct ferric reducing ability plasma (FRAP) experiment, iron (III) sulphate, heptahydate, sodium acetate trihydrate, glacial acetic acid, hydrochloric acid (37%, analytical reagent grade, fisher Scientific), tripyridyltriazine (TPTZ), and iron (III) chloride, Hexahydrate were bought from VWR international Laboratory Chemicals. Anhydrous sodium hydroxide, nitric acid (65%, merck kommanditgesellschaft auf aktien), pphosphate monodibasic, Potassium phosphate dibasic, ammonium chloride, magnesium sulphate heptahydrate, potassium chloride, and soduim acetate were bought from VWR International Laboratory Chemicals and used to prepare the synthetic wastewater. Distilled and milli-Q water were used as required. Phosphate, Nitrate and COD reagent were bought from Hach Lange and used to determine synthetic wastewater characteristics before and after adsorption.

General flow of experimental procedure

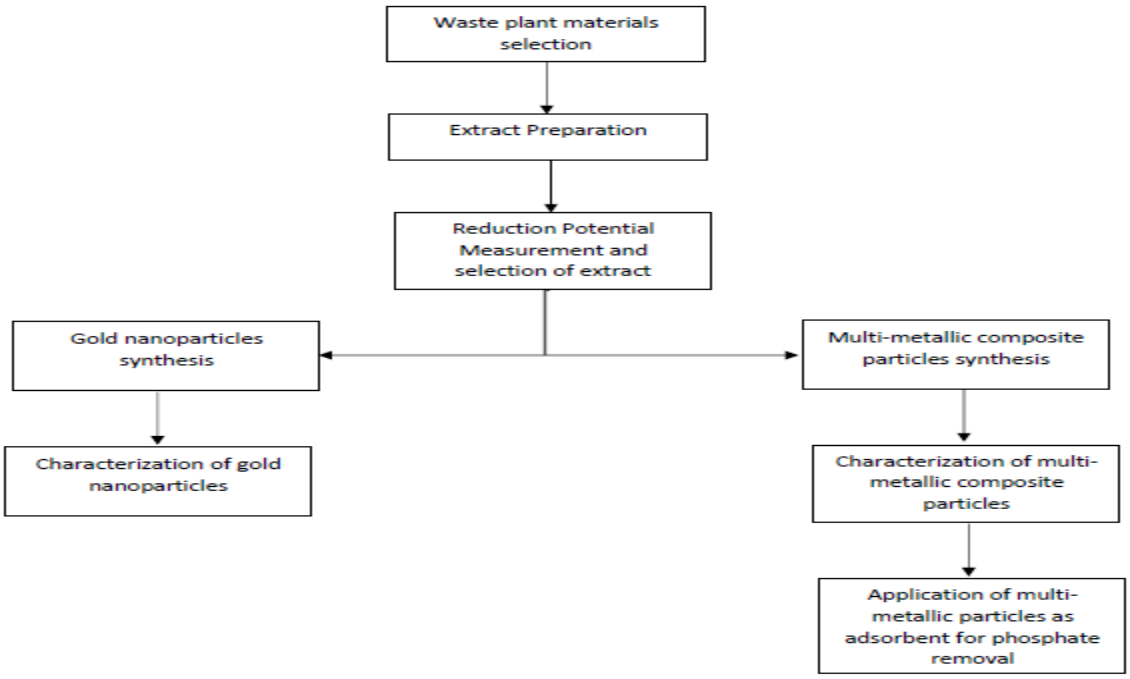

Figure 2 General flow of the experimental procedure

2.2 Waste plant materials selection and collection

Various waste plant materials were collected from Algarve region. Waste plant materials were selected based on the availability and the cost of the plant material (plant materials with less cost were given priority). Waste raspberry leave (dried and wet), waste raspberry fruit from National Fruit Company and prickly pear and carob were collected in the Algarve region. The fresh leaves of raspberry were washed 3 times with distilled water to remove any dirty and dried in an oven at 40 ^{o}C for 48 hours (only for the dried leaves). The plant biomass was crushed using a mechanical crusher to get the powder and the fruit part was crushed manually using crushing equipment.

2.3 Extract preparation

20 g of each selected plant materials mentioned above were used for preparation of the extract. The extract were prepared by boiling the mixture of 20 g of the plant material in 150 ml mixture of water-ethanol (50:50, v/v) used as extracting agent in 250 ml glass bottle in water bath at 60 ^{o}C for 30 minutes. The extraction conditions were selected taking into account information from literature values and the sustainability and feasibility of the process (Bappi Paul, 2015; K. Anand, 2015; Sathishkumar G., 2016). The prepared extract was filtered using a Whatmann filter paper nº 1 and stored at 4 ^{o}C for future use. The pH of the extract was measured using a pH meter (GLP 21, Crison). The flow chart below (fig. 3) shows the extract process.

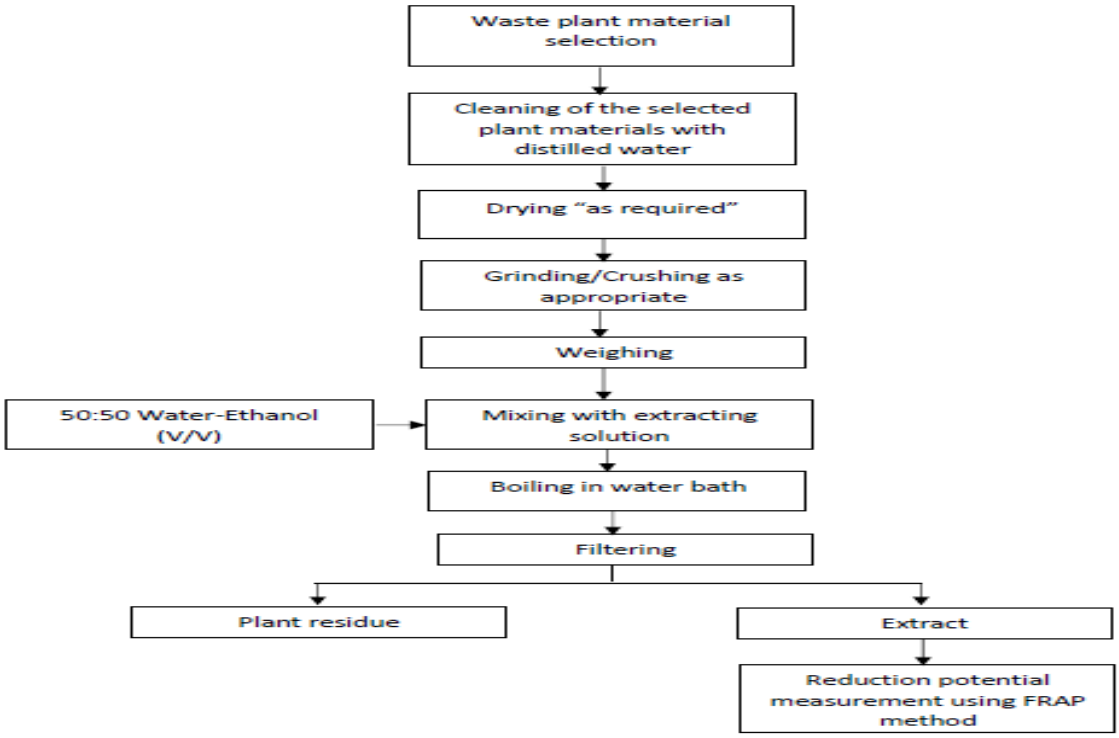

Figure 3 General flow chart of the extraction process.

2.4 FRAP method for measuring reduction potential

Ferric reducing ability plasma (FRAP) method is simple, automated test measuring the ferric reducing ability of plasma, presented as a novel method for assessing "antioxidant power." Ferric to ferrous ion reduction at low pH causes a colored ferrous-tripyridyltriazine complex to form. FRAP values are obtained by comparing the absorbance change at 593 nm in test reaction mixtures with those containing ferrous ions in known concentration. Absorbance changes are linear over a wide concentration range with reducing compounds (Iris F. F. Benzie, 1996).

FRAP method was used for measuring the reduction potential of selected plant material. For that purpose 1.00 mM Fe^{+2} stock aqueous solution was prepared by dissolving 0.1390 g of $FeSO_4.7H_2O$ into 500 ml distilled water and then from that one various iron (II) solutions with concentration in the range of 0.10-1.0 mM (0.10, 0.20, 0.40, 0.60, 0.80, 1.0 mM) were prepared for calibration according to table 3 below. Aliquots of 0.20 mL of each standard solution were pipetted to Eppendorf's and placed in ice before being used.

Table 3 Preparation of Fe^{+2} standard aqueous solutions

Standard concentration	$FeSO_4.7H_2O$ Solution	Distilled water
mM	(ml)	(ml)
0.10	1	9
0.20	2	8
0.40	4	6
0.60	6	4
0.80	8	2
1.0	10	0

2.4.1 FRAP reagent preparation

A buffer solution with a pH of 3.6 was prepared by dissolving 1.55 g of sodium acetate trihydrate in 8 ml glacial acetic acid followed by addition of distilled water until final volume of 500 ml. A solution of 40mM HCl was prepared by dissolving 0.73 ml of 37% HCl in 500 ml of distilled water. Fresh solution of 10 mM tripyridyltriazine was prepared by dissolving 0.031 g of tripyridyltriazine in 10 ml of 40mM HCl at 50 ^{o}C. Fresh ferric (III) chloride, hexahydrate (20 mM) was prepared by dissolving 0.054g of $FeCl_3.6H_2O$ into 10ml of distilled water. The FRAP reagent was prepared in a flask by mixing the above mentioned prepared solutions according to the following proportions: 100ml of acetate buffer at pH 3.6, 10 ml of 10 mM TPTZ, 10 ml of 20 mM of $FeCl_3.6H_2O$, 12 ml of distilled.

2.4.2 Reduction potential measurement

A blank sample was prepared by mixing 30 µl of distilled water-ethanol (50:50, v/v) in cuvettes and then 1ml of the FRAP reagent was added vigorously into the same cuvettes. After 4 minutes the absorption of

the blank it was read with UV-Vis spectrophotometer (DR 2800, HACH LANGE) at 595nm and the reading was made to be zero before the reading of each standard and sample. Then 30 µl of each standard was added in cuvettes and 1 ml of FRAP reagent was added vigorously to each of the standard solution. The absorbance was read after 4 minutes. Finally 30 µl of each extract was added in cuvettes and 1 ml of the FRAP reagent was vigorously added to each of the extract. The absorbance was recorded after 4 minutes. Triplicate analysis was done for each experiment.

2.5 AuNPs synthesis using raspberry leave extract

In the typical experimental method, a standard gold(III) chloride solution from Sigma-Aldrich, gold atomic spectroscopy standard concentrate, 1.00 g/L Au standard solution was used to prepare 50 mL standard solutions of 25 mg/L, 50mg/L, 75 mg/L and 100 mg/L, which were placed in 250 ml flask. 5 mL raspberry leave extract were added drop by drop to each flask at room temperature while it was shaking at 100 rpm with a shaker (TH 15, Edmund Buhler). Different synthesis time 0 min (at the very beginning of the reaction), 5 min, 10 min, 15 min, 30 min and 60 min were monitored using UV-Visible spectrophotometery (BIOTEK, Synergy spectrometer) by measuring the absorbance between 400-800 nm, the range aims to analyze the surface plasmon resonance (SPR) peak. Different concentrations of gold (III) solution and synthesis times were used to get the optimum condition and other initial condition were selected based on literature review (Bappi Paul, 2015; Chun-Gang Yuan, 2017; Jia Yu, 2016).

After synthesis following the mentioned conditions, the particles were separated from the solution by centrifugation at 4000 rpm for 25 minutes using centrifuge (scientific K3 serious) at 4000 rpm for 25 minutes. Then the supernatant was separated from precipitate by manual decantation and the precipitate was dried in a desiccator overnight. The Au-(III) concentration in the initial standard gold (III) solution and in the supernatant was analyzed for Au-(III) concentration using a MP-AES (Agilent 4200 MP-AES, Santa Clara, CA). The pH was measured using a pH meter (GLP 21, Crison). Triplicate analysis was done for each test. The best optimum condition was selected for synthesis of AuNPs.

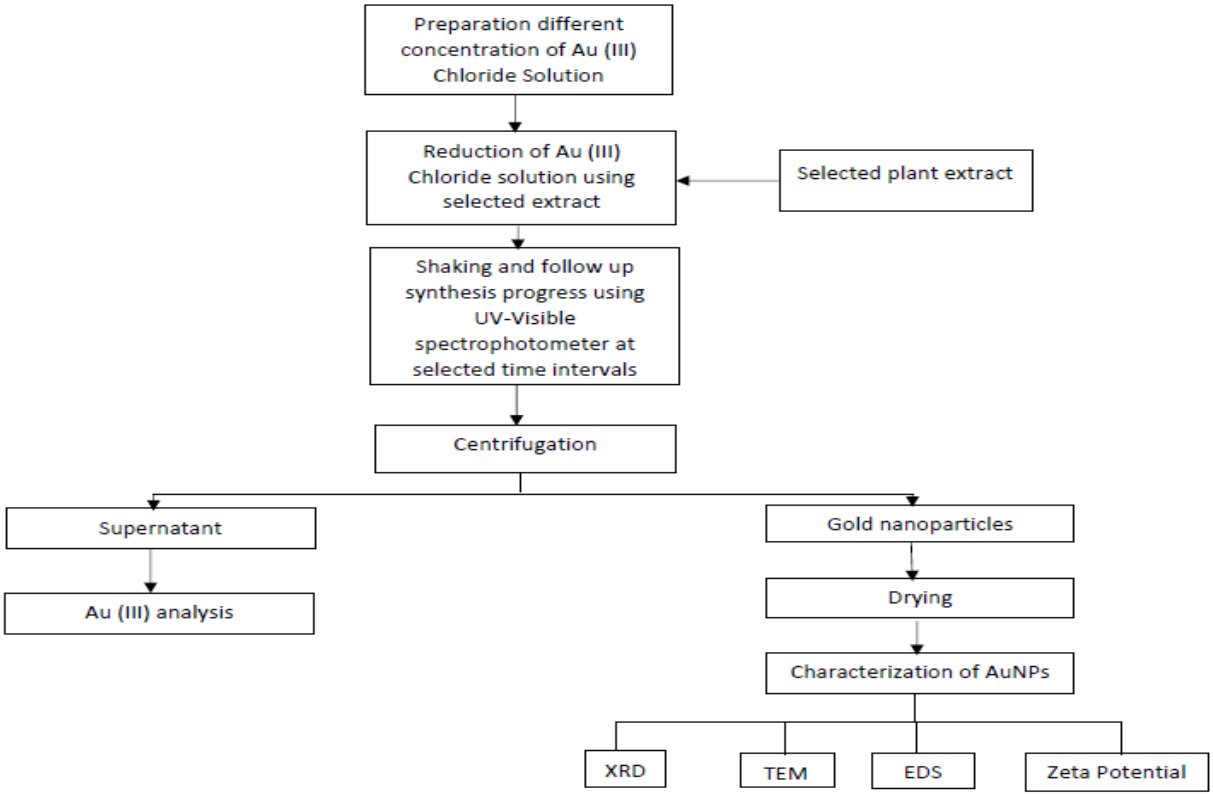

Figure 4: General flow chart for gold (0) synthesis

2.6 Synthesis of multi-metallic composite particles

2.6.1 Collection and characterization of acid mine drainage

Acid mine drainage wastewater was collected from São Domingos at São Domingos mining area. The characterization of the wastewater was done using MP-AES (Agilent 4200 MP-AES, Santa Clara, CA) and flame atomic absorption spectroscopy (FAAS) (novAA 350, analytikjena). Selected main metallic components Fe, Al, Zn, Cu, based on preliminary study, were analyzed. The pH of AMD was measured using pH meter (GLP 21, Crison).

2.6.2 Synthesis of multi-metallic composite particles using raspberry leave extract

The multi-metallic composite particle synthesis process was optimized in terms of wastewater-extract ratio (v/v) and different synthesis time. Wastewater-extract ratios (v/v) of, 75:25, 85:25, 95:5 and different synthesis time of 0.5h, 1h, 2h, 3h, and 6h were investigated. Based on the ratio mentioned volume of acid mine drainage wastewater was placed in 250 ml glass bottle and a certain volume of raspberry leave extract was measured and added drop by drop to each bottles at room temperature while bottles were shaking at 100 rpm on a shaker (TH 15, Edmund Buhler). 5 ml of solution was collected from each bottle at different time intervals: 0.5h, 1h, 2h, 3h, 6h and centrifuged at 14000 rpm

for 20 minutes (ROTOFIX 32, hettich zentrifugen,). Then the precipitate and supernatant were separated by manual decantation. The precipitate was dried in a desiccator overnight. The initial concentration Al, Fe, Zn and Cu of AMD and the filtrate were analyze using FAAS (novAA 350, analytikjena) and MP-AES (Agilent 4200 MP-AES, Santa Clara, CA). The pH was measured using pH meter (GLP 21, Crison). Considering the sustainability and feasibility of the process, the conditions in terms of wastewater-extract (v/v) ratio and reduction time that allow obtaining the highest metal reduction percentage was used for production composite particles. Triplicate analysis was done for each experiment. The general synthesis method was shown in fig. 5 below.

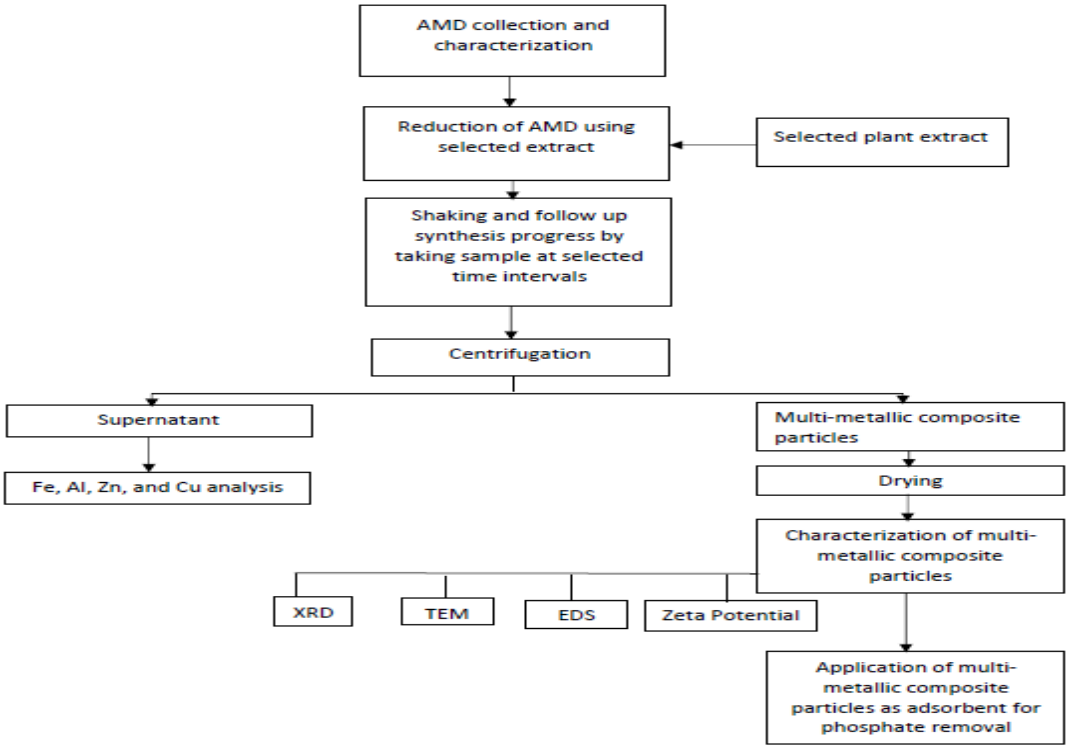

Figure 5: General flow chart for synthesis of multi-metallic composite particles

2.7 Characterization of AuNPs and multi-metallic composite particles

The characterization (size, shape, morphology, surface area, crystal structure, elemental composition, surface charge and stability) of AuNPs and multi-metallic composite particles were done using transmission electron microscopy (TEM), energy-dispersive X-ray spectroscopy (EDS/EDX), X-ray diffraction (XRD), and zeta potential. The formation AuNPs were monitored using UV-Vis spectrophotometer in a range between 400-800 nm.

2.7.1 UV-Vis spectrophotometer

The formation AuNPs were monitored using UV-Vis spectrophotometer (BIOTEK, Synergy) in a range between 400-800 nm.

2.7.2 Transmission electron microscopy (TEM)

The images of AuNPs and multi-metallic composite particles were recorded with TEM for determination of the shape, and size of the particles and diffraction.

2.7.2 Energy-dispersive X-ray spectroscopy (EDS/EDX)

The elemental composition of AuNPs and multi-metallic composite particles was determined using EDS coupled with TEM.

2.7.3 X-ray diffraction (XRD)

The crystallographic structures of obtained AuNPs and multi-metallic particles were analyzed by X-ray diffraction (XRD) using a PANalytical XPERT-PRO powder diffractometer operating at 45 kV and 30 mA with Cu Ka radiation filtered by Ni. The XRD patterns were recorded using an X'Celerator detector with a step size (2θ) of 0.03^{o} and a time per step of 1000 s. Peak analysis and the identification of crystalline phases were based on comparison using High-Score Plus software with the ICDD PDF-2 database. From the width of the XRD peaks the crystallite size was calculated by using Scherrer's equation below,

$$\tau = \frac{K\lambda}{\beta\cos\theta} \quad (1)$$

Where,

τ is the mean size of the ordered (crystalline) domains, which may be smaller or equal to the grain size;

K is a dimensionless shape factor, with a value close to unity. The shape factor has a typical value of about 0.9, but varies with the actual shape of the crystallite;

λ is the X-ray wavelength;

β is the line broadening at half the maximum intensity (FWHM), after subtracting the instrumental line broadening, in radians. This quantity is also sometimes denoted as Δ(2θ);

θ is the Bragg angle (in degrees).

2.7.4 Zeta potential

The Zeta potential measurements of AuNPs and multi-metallic particles were performed using Malvern Nano Zetasizer (Nano-Z590, Nano Series) equipment at 146 mV, by adding the precipitates to aqueous solutions prepared using Milli-Q water with different pH from 1 to 12. Immediately after the particles addition, the solution was submitted during 5 minutes ultrasound (FB15054, Fisherbrand) treatment. The pH of the Milli-Q water was adjusted using 5% NaOH or 5% HNO_3 as required.

2.8 Application of multi-metallic composite particles as adsorbent for phosphate removal

Synthetic wastewater with intended specific concentration of pollutant was prepared by mixing component 1 and component 2 (table below). It was prepared by mixing 20 ml of component 1 and 20 ml of component 2 into 1.3 ml of tab water and total volume was 1.6 L.

Table 4: Component 1, Media A.

Chemicals	**Amount weighed for 1 L of distilled water (g)**
Sodium Acetate	51.68
Magnesium sulphate heptahydrate	8.87
Potassium chloride	3.50

Table 5: Component 2, Media B.

Chemicals	**Amount weighed for 1 L of distilled water (g)**
Ammonium Chloride	18.94
Potassium phosphate dibasic	7.33
Potassium phosphate monobasic	2.86

The produced multi-metallic composite particles were used as adsorbent to test the remove phosphate from synthetic wastewater. The adsorption experiments were carried out in batch system using an adsorbent dosage of 1 g/L and 500 mg/L by adding 20 mg and 10 mg of the multi-metallic composite particles to 20 mL of synthetic wastewater respectively in 250 mL glass bottle. The solutions were shaken at 100 rpm on a shaker (TH 15, Edmund Buhler) at room temperature. The phosphate concertation at initial and at different time intervals, 0.5 hr, 1 hr, 2 hr, 3 hr, 6 hr and 12 hr, were analyzed for phosphate concentration by molecular UV-Vis spectrophotometry at 880 nm according to 490 p react procedure using spectrophotometer (DR 2800, HACH LANGE). The initial concentration of nitrate and COD were also measured using molecular UV-Vis spectrophotometry (DR 2800, HACH LANGE) at 345 nm and 350nm respectively. 2ml sample from the reactor bottle was collected after stopping the shaker for 2 minutes and letting the particles settle to the bottom of the bottle. To make sure that all of the adsorbent was removed from the sample, all the samples were centrifuged (HERAEUS FRESCO 17, Thermo scientific) at 13,000 rpm for 1 minute. 20 ml blank of synthetic wastewater was used as a control during this experiment. Pollutant removal efficiency was optimized based on adsorbent dosage and adsorption time to get the condition for best pollutant removal efficiency.

2.9 Removal efficiency

The metal removal or reduction efficiency was presented as percentage of metal removal of the extract and it was calculated based on the initial metal concentration and the concentration metal concentration at a fixed synthesis time according to the following equation.

$$Removal\ efficiency(\%) = (\frac{Ci-Ct}{Ci} \times 100) \quad (2)$$

Ci initial concentration of metal ion the solution, *Cf* final concentration of the metal ion after synthesis using raspberry extract

The removal efficiency of phosphate, expressed as percentage of phosphate removal, was calculated based on the initial phosphate concentration and on the concentration of phosphate at certain fixed time.

$$Removal\ efficiency(\%) = (\frac{Ci-Ct}{Ci} \times 100) \quad (3)$$

Ci initial concentration of phosphate, *Ct* concentration of phosphate after certain time

2.10 Statistical analysis

Triplicate analysis was done and the data expressed as mean ± confidence interval at 95% confidence level as required. Statistically significant differences between the results were obtained by carrying out analysis of variance (one-way ANOVA) at 95% confidence level. All statistical analyses were carried out using the excel spreadsheet, 2016 software.

3. Results and Discussions

3.1 Reduction potential of selected plant materials

The first step in the synthesis of AuNPs and multi-metallic composite particles was the selection of waste plant materials and its extract with the best reduction potential and based on its availability and cost of the material. Waste raspberry leave, waste raspberry fruit, carob and prickly pear were selected. These materials were considered as waste from agricultural activity and abundant in Algarve region, therefore they can also be considered as low cost. This feature makes them very attractive from different perspectives such as an option for waste management and reuse.

FRAP method were used for measuring the reduction potential of the waste plant materials. In our experiment 1.00 mM stock standard ferrous ion concentration was prepared by dissolving 0.139 g of $FeSO_4.7H_2O$ and various concentration in the range of 0.10-10 mM (0.10, 0.20, 0.40, 0.60, 0.80, 1.0 mM) were prepared for calibration from the stock solution.

The result in the fig. 6 below revealed dried raspberry leave has the highest reduction potential whereas prickly pear has lowest reduction potential. The highest reduction potential of dried raspberry leave might be due to the extract contain relatively high amount of different compounds such as terpenoids, phenols, proteins, carbohydrates, tannins, saponins, proteins, and reducing sugar (Palaniselvam Kuppusamy M. M., 2016; Rani Mata, 2016; Jayanta Kumar Patra, 2016; Sathishkumar G., 2016; Amit Kumar Mittal, 2013; K. Anand, 2015).

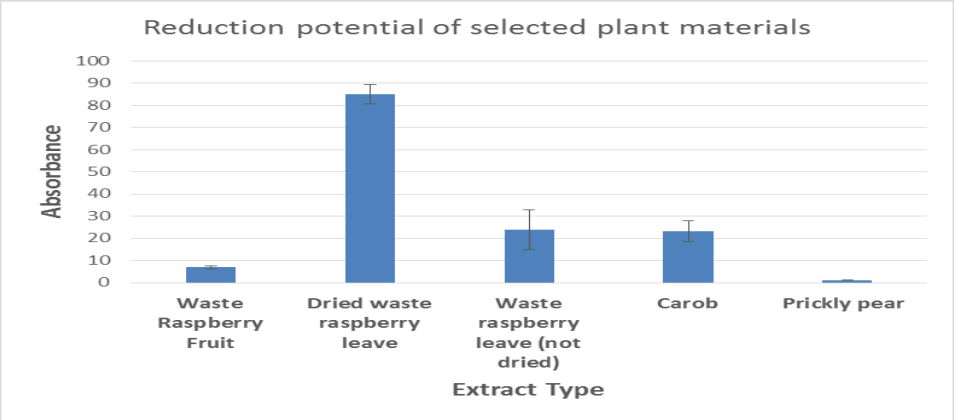

Figure 6 Reduction potential of selected plant materials.

Based on the reduction potential, sustainability and feasibility of the process, dried leave raspberry extract was selected for the synthesis of AuNPs and multi-metallic composite particles.

3.2 Synthesis of gold nanoparticles and multi-metallic composite particles

In our experiments the synthesis of gold nanoparticles and multi-metallic composite particles was prepared in single pot by simply mixing the extract with an aqueous solution containing the precursor metal ion at room temperature. Generally the synthesis was completed within short period of time but it was required to monitor the synthesis progress to determine the optimized time of synthesis (Chun-Gang Yuan, 2017; Amit Kumar Mittal, 2013). The synthesis progress was monitored and the results are discussed below.

Biomolecules present in plant extracts might reduce metal ions to zero valent nanoparticles in a single-step and green synthesis process. This biogenic reduction of metal ion is quite rapid, readily conducted at room temperature and pressure, and easily scaled up. The reducing agents might involve are various plant compounds (such as - alkaloids, phenolic compounds, terpenoids, amines, flavonoids, water soluble heterocyclic components as well as tannins, saponins, proteins, reducing sugars and other metabolites) (Amit Kumar Mittal, 2013; Bappi Paul, 2015; Chun-Gang Yuan, 2017).

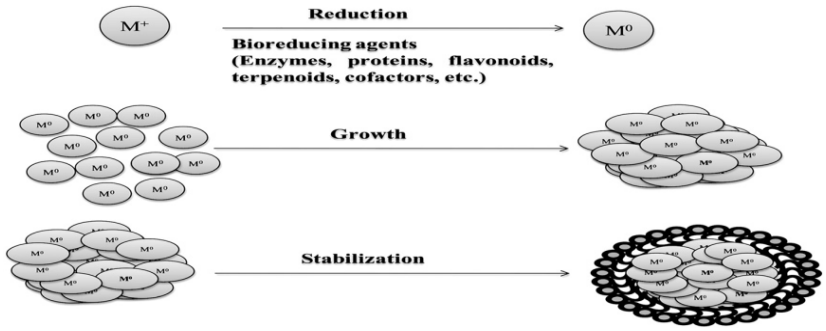

Figure 7 Mechanisms of metal nanoparticle synthesis (M^+-metal ion) *(Amit Kumar Mittal, 2013)*.

3.3 Ultraviolet-visible (UV-Vis) spectroscopy analysis

After the addition of the extract to the gold- (III) solution of various concentrations (25 mg/L, 50 mg/L, 75mg/L, 100 mg/L) following the procedure mentioned in the experimental part, the color of the solution immediately changed from light yellow to amber and finally turn into dark violet (see fig. 8 below) suggesting the formation AuNPs. The color changes indicated that Au-(III) was reduced to Au (0) by biomolecules present in the extract (Chun-Gang Yuan, 2017; Bappi Paul, 2015; Palaniselvam Kuppusamy M. M., 2016; Masumeh Noruzia, 2011) and also indicate the occurrence of a redox reaction whereby Au (III) ions are reduced to Au (0) by the plant components, which are in turn oxidized to other species (K. Anand, 2015). Although the actual mechanism is not well understood, plant extract might have components such as phenolics, polyols, amines, flavonoids, water soluble heterocyclic components as well as tannins, saponins, gallic acids, proteins, reducing sugars and other metabolites, which may have the ability to act as reducing agents (Palaniselvam Kuppusamy M. M., 2016; Rani Mata, 2016; Jayanta Kumar Patra, 2016; Sathishkumar G., 2016; Amit Kumar Mittal, 2013; Akbar Soliemanzadeh, 2017; K. Anand, 2015).

Standard Au (III) chloride solution

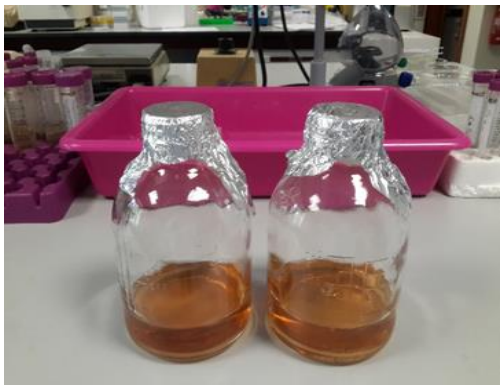

-Solution immediately after extract addition

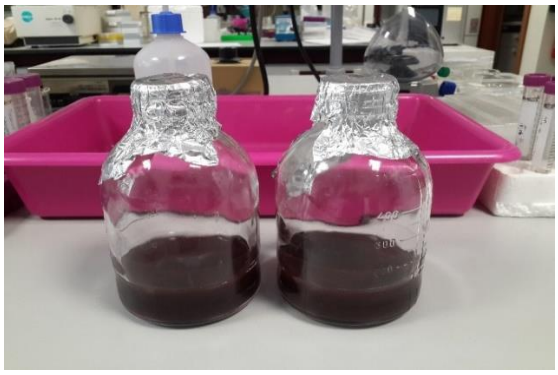

Solution after 15 minutes synthesis time

Figure 8 Color change progress before and after addition of extract to the Au-(III) solution.

The formation of AuNPs and the synthesis stages were further monitored by molecular UV-Vis spectrometry (BIOTEK, Synergy) between 400-800 nm at different time: 0 min (immediately after extract addition), 5 min, 10 min, 15 min, 30 min and 60 min (fig. 9 below). There was no further color change in the solution and no SPR peak increase after 15 minutes, which may indicate that the formation of AuNPs is completed within 15 minutes for all standard Au-(III) chloride concentration (25mg/L, 50 mg/L, 75 mg/L, 100mg/L). The maximum SPR peak of AuNPs were observed at 540 nm, 550nm, 555nm, 565 for the standard Au-(III) concentration of 25mg/L, 50 mg/L, 75 mg/L and 100 mg/L, respectively (Fig.9).

The Au-(III) solution with 100 mg/L gave the highest SPR peak whereas the 25mg/L gave the lowest one. The absorbance peak was increased steadily as the initial Au-(III) concentration increased in the reaction and also as the time of the synthesis increased until 15 minutes. However, after 15 minutes there was no increase of the SPR peak. Thus, from the optimization study we have concluded that an increase in the initial concentration of Au-(III) solution resulted in an increase in the available ions for reduction which caused an increase the number of synthesized nanoparticles (Nabeel Ahmad, 2017) . On other hand, an increase in the intensity of the SPR peak with time clearly suggested gradual increase yield of the nanoparticles with time (Bappi Paul, 2015; K. Anand, 2015). The position and shape of SPR peak of NPs are strongly dependent on particle size, dielectric medium and surface adsorbed species (Pannerselvam Balashanmugama, 2016).

Similar result was reported on time-dependent UV–vis spectra of AuNPs which showed SPR band around 550 nm after 1h. After 12 hours SPR peak red shifted and appeared around 555nm. This red-shift along with steady increase in intensity of SPR peak clearly suggested gradual increase of size and yield of the NPs with time (Bappi Paul, 2015). Similar SPR peak, range between 540 nm and 560 nm, was reported during the synthesis of AuNPs using various leaf extracts (Bappi Paul, 2015; Chun-Gang Yuan, 2017; Pannerselvam Balashanmugama, 2016; K. Anand, 2015).

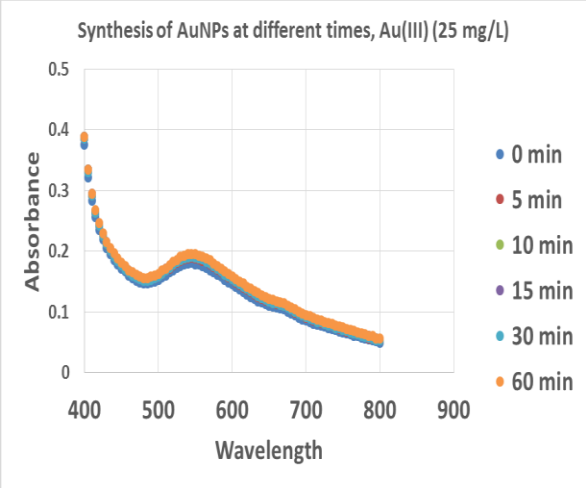

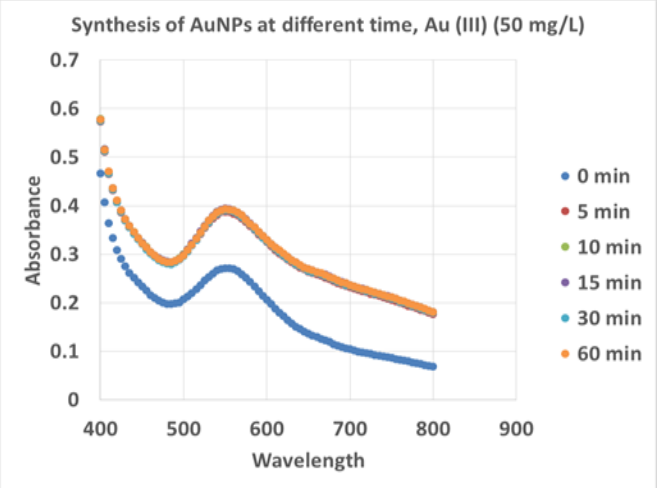

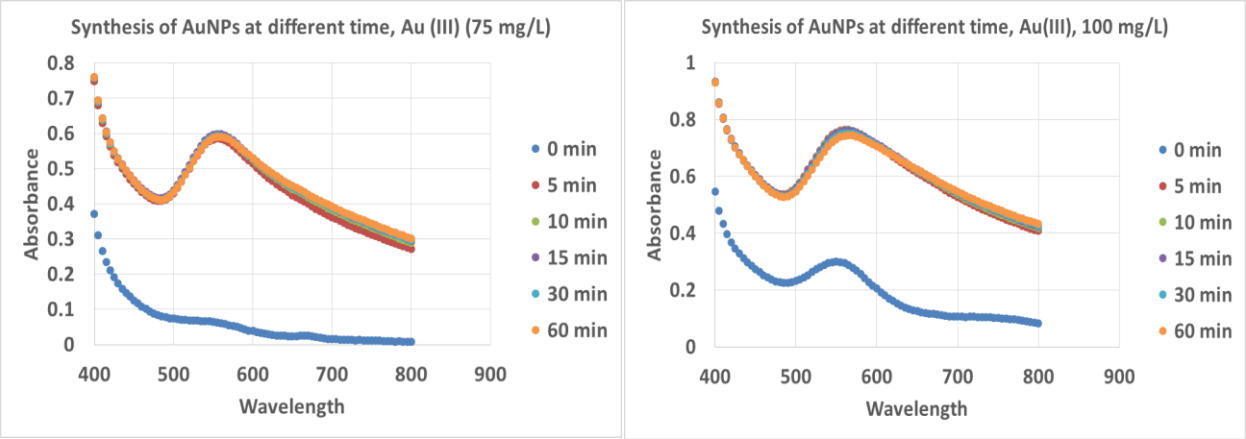

Figure 9 UV-Vis synthesis progresses of AuNPs at different time and concentration.

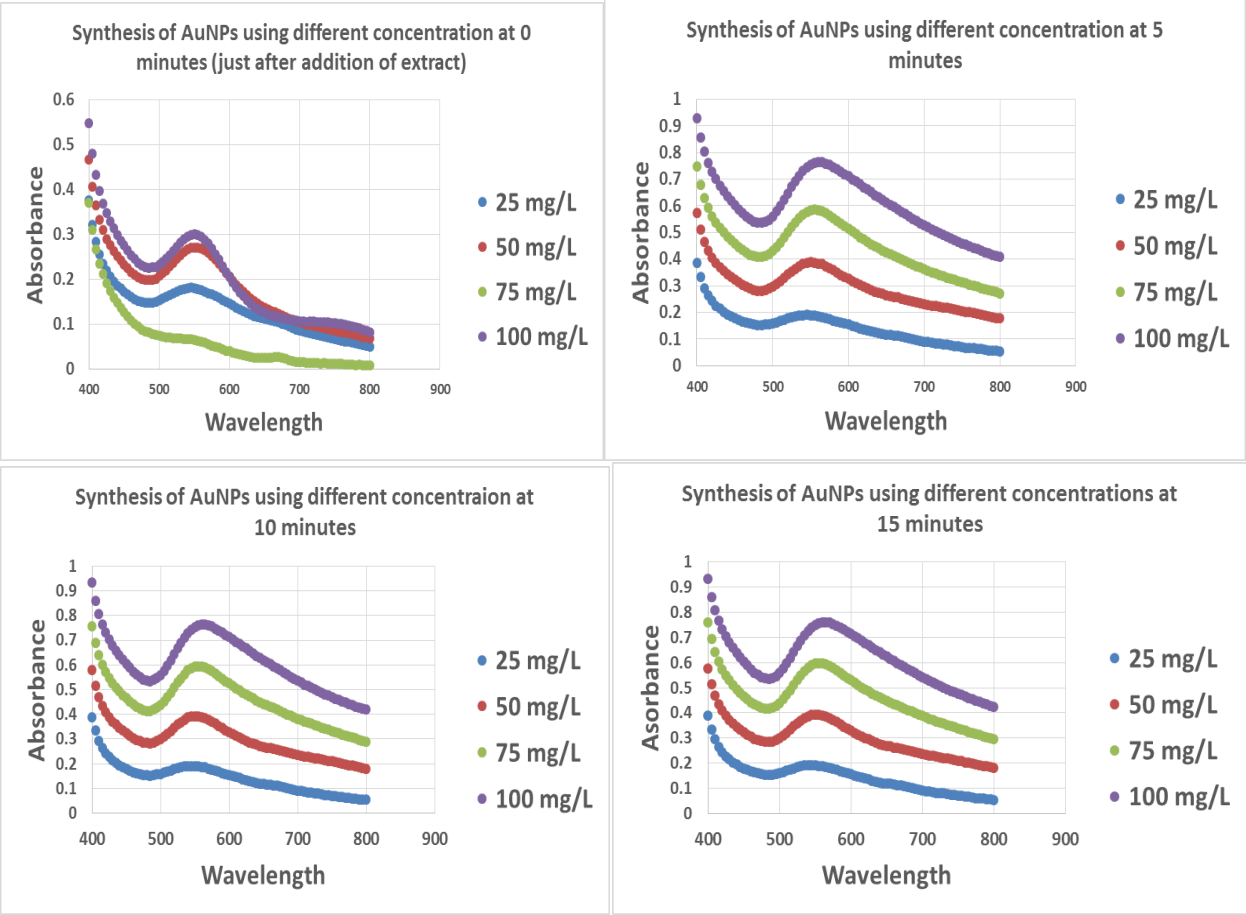

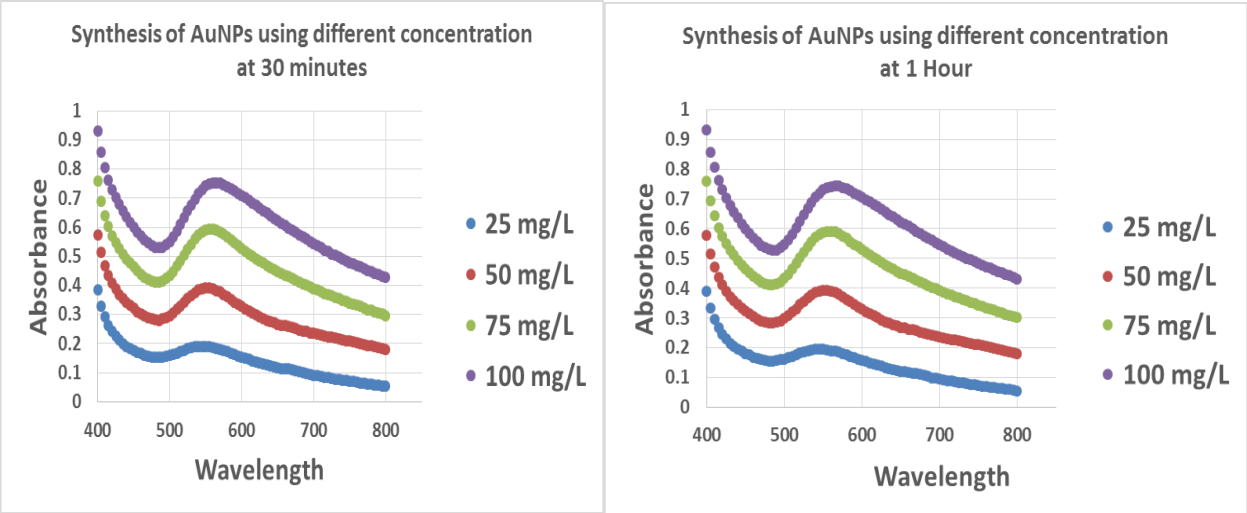

Figure 10 UV-Vis comparisons between different synthesis time and concentrations of Au-(III) chloride solution.

The result from UV-Vis spectrophotometry indicated that 100 mg/L Au-(III) chloride solution and 15 minutes synthesis time was the best synthesis conditions (figure 9 and 10). The selection was based of the sustainability, feasibility and formation of higher yield of AuNPs (figure 9 and 10). More NPs were synthesized using the selected optimum conditions and the particles were separated from the solution by centrifugation. After centrifugation, the supernatant was decanted manually into another falcon for residual Au - (III) analysis, and the particles were dried overnight in desiccator. The dried particles were formed golden film (fig. 11 below) and small precipitates on the side wall and the bottom of the falcon. These particles were used for the characterization of AuNPs.

Figure 11 Gold film and precipitate on the side wall and bottom of falcon.

The reduction efficiency of selected extract was measured by analyzing the concentration Au-(III) in the solution before and after AuNPs synthesis. The reduction efficiency is shown in the table 6 below. The highest reduction efficiency achieved was 95 % using the optimum conditions: 5 ml of extract in 50 ml of 100 mg/L Au-(III) solution (v/v) at 15 minutes synthesis time. The high reduction potential in short period of time might be due to the presentence of different biomolecules which strongly involved in the reduction process. Similar AuNPs synthesis trend using plant extracts was reported in various studies (Amit Kumar Mittal, 2013; H. Joy Prabu, 2015; Jasmine Jacob, 2012; María Martínez-Cabanas, 2016; Khwaja Salahuddin Siddiqi, 2017; Palaniselvam Kuppusamy M. M., 2016).

Table 6 Reduction efficiency of dried raspberry leaves extract.

Initial concentration of Au (III) chloride solution (mg/L)	Final supernatant concentration of Au (III) chloride solution (mg/L)	Reduction efficiency (%)
112 ± 11	5.0 ± 2.5	95.0 ± 0.6

3.4 Synthesis of multi-metallic composite particles

3.4.1 Characteristics of acid mine drainage

The main chemical composition and characteristics of the AMD wastewater are summarized in table 7 below. The wastewater has relatively high concentration of aluminum and iron, whereas low concentration of copper and zinc. It was highly acidic with low average pH.

Table 7 Composition of AMD sample from São Domingo's mine site in terms of main metals and pH

Composition of acid mine drainage wastewater				
pH	Al (mg/L)	Fe (mg/L)	Cu (mg/L)	Zn (mg/L)
2.5 ± 0.1	229 ± 3	200 ± 10	33 ± 3	40 ± 3

3.4.2 Synthesis of multi-metallic composite particles using dried raspberry leave extract

The first indication of successful multi-metallic composite particle formation was the appearance of a black color (Fig. 12 below). This was a rapid reaction as indicated by the immediate color change on mixing the AMD wastewater with extract of dried raspberry leave. This color change may validate the occurrence of a redox reaction whereby metal (+) ions are reduced to metal (0) by the plant components, which are in turn oxidized to other species. Or there might be other form reactions which result in precipitate (K. Anand, 2015). After the synthesis, the solution was centrifuged and black multi-metallic composite particles were produced (fig. 14 below).

Figure 12 AMD wastewater before (left) and after (right) addition of plant extract

In comparison with other metals removal efficiency, high removal efficiency was observed for iron (85-90%) whereas lower removal efficiency (25-30%) for aluminum, copper and zinc at wastewater-extract ratio of 75:25 (v/v) ratio and 3h and 6 h synthesis time (figure 13). Lower removal efficiency was observed at wastewater-extract ratio of 85:15 (v/v) and 95:5(v/v), and at the early stage of synthesis time. The high removal potential as the ratio (v/v) increased in favor of the extract might be related to the presence of enough compounds such as phenolic, alkaloids, flavonoids in the extract (Rani Mata, 2016; Jayanta Kumar Patra, 2016; Sathishkumar G., 2016; Akbar Soliemanzadeh, 2017; K. Anand, 2015).

The highest removal efficiency of iron might be due to the compounds in the plant extract strongly involved in iron removal comparing to the other mentioned metals (Palaniselvam Kuppusamy M. M., 2016). Generally the removal efficiency increased as the time increased for all wastewater-extract (v/v) ratios. However, there was no significant difference in terms of metal removal efficiency between 3 h and 6 h of contact between the extract and AMD, for all AMD-extract ratios (v/v). In comparison these results to other treatment methods such as biochemical passive reactors, utilization of residue gas sludge (BOS sludge), traditional neutralization (Yaneth Vasquez, 2016; A. Jafaripour, 2015; Olivier Lefebvrea, 2012), the removal efficiency for iron was very good and promising. But the removal efficiency for aluminum, copper and zinc was low. Even though the removal efficiency was low, our intension was recovery of multi-metallic composite particles which could possibly use for the treatment of other wastewater as adsorbent. In fact, removal of metals using plant extract could potentially apply as pretreatment option for wastewater contaminated with metals.

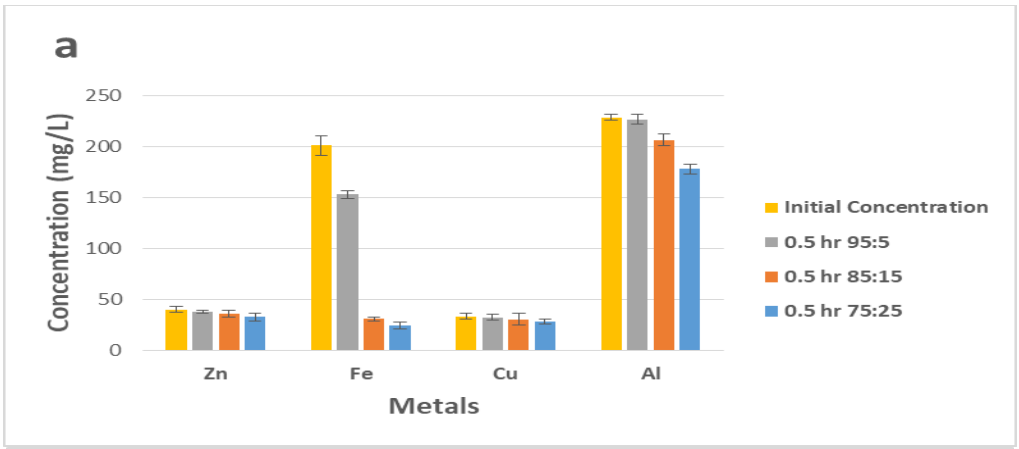
a
Concentration (mg/L)
250
200
150
100
50
0
Zn
Fe
Cu
Al
Metals
Initial Concentration
0.5 hr 95:5
0.5 hr 85:15
0.5 hr 75:25

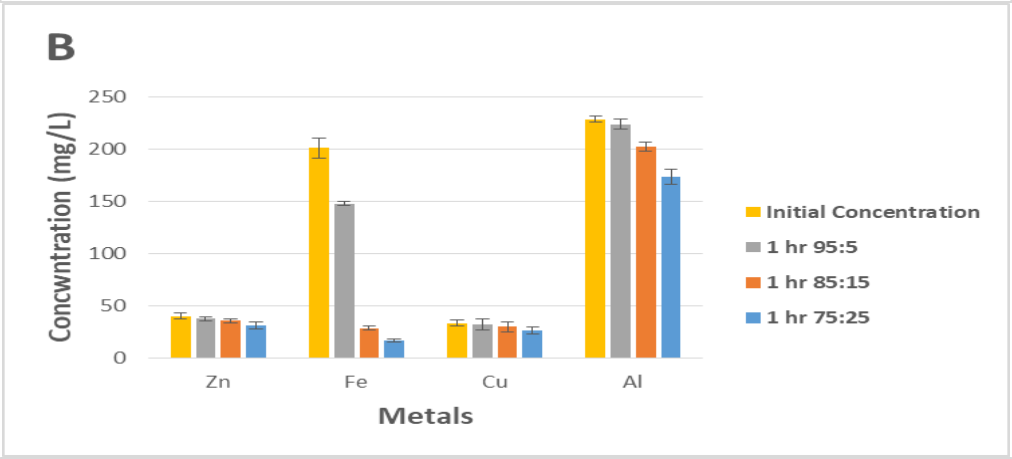
B
Concwntration (mg/L)
250
200
150
100
50
0
Zn
Fe
Cu
Al
Metals
Initial Concentration
1 hr 95:5
1 hr 85:15
1 hr 75:25

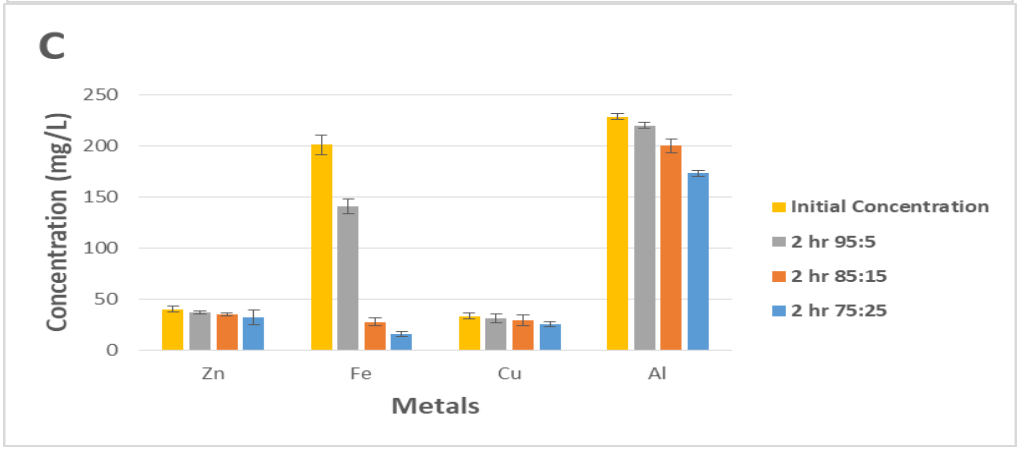
C
Concentration (mg/L)
250
200
150
100
50
0
Zn
Fe
Cu
Al
Metals
Initial Concentration
2 hr 95:5
2 hr 85:15
2 hr 75:25

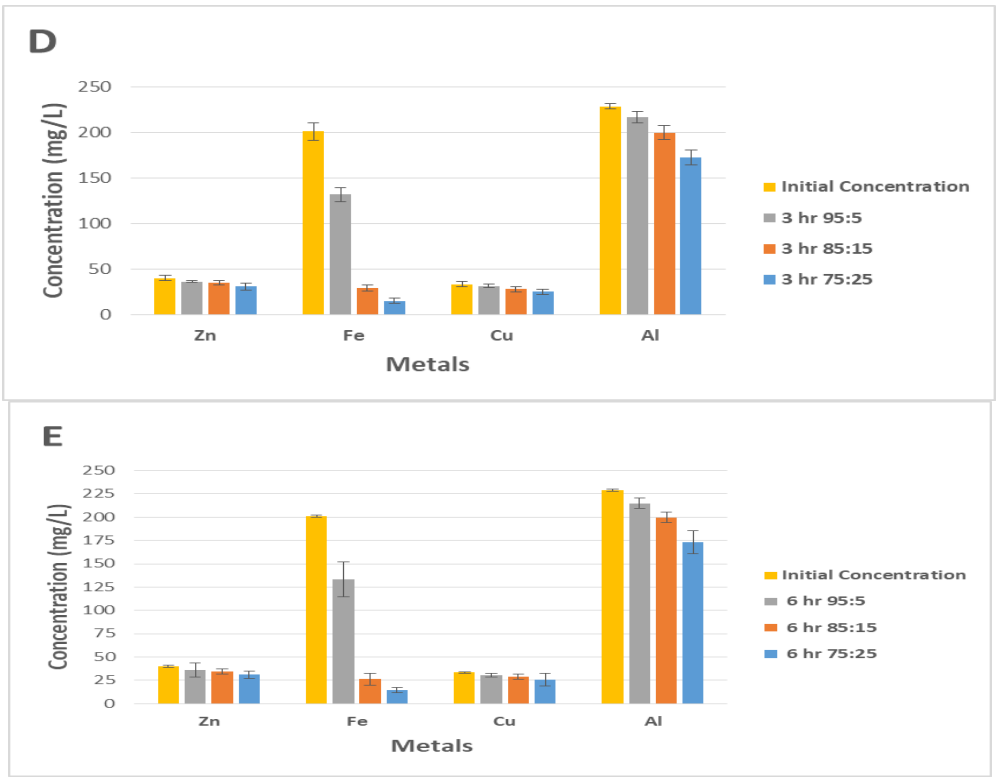

Figure 13 Initial and final concentrations of metals after extract addition at different time and mixing ratio. (A) 0.5 h, (B) 1h, (C) 2h, (D) 3h, (E) 6h.

The optimum conditions were selected based on feasibility, sustainability and amount of particles produced. After the optimum conditions were selected, which was 3 h synthesis time and 75:25 (v/v) AMD wastewater-extract ratios, more multi-metallic composite particles were synthesized following the procedure indicated in the experimental part. The synthesized particles were used for characterization of multi-metallic composite particles and for phosphate removal via adsorption.

Figure 14 Multi-metallic composite particles.

3.5 X-ray diffraction (XRD) analysis

The characteristic X-ray diffraction pattern generated in a typical XRD analysis provides a unique "fingerprint" of the crystals present in the sample. When properly interpreted, by comparison with standard reference patterns and measurements, this fingerprint allows identification of the crystalline form (C. Suryanarayana, 1998).

The XRD pattern revealed the crystalline nature of the synthesized AuNPs (figure 15 below). The sharp intense peaks of Bragg reflections corresponding to (111), (200), (220), (311) and (222) planes at 2θ values of 38.2^0, 44.5^0, 64.7^0, 77.7^0 and 81.2^0, respectively, displays the crystalline nature of AuNPs. These planes represent cubic structure of the AuNPs in comparison with High-Score Plus software with the ICDD PDF-2 database. No other peaks were observed due to impurities, which confirmed the synthesized particles were purely AuNPs. The mean size of the crystallite was calculated using the Scherrer's equation by determining the width of the (111) Bragg's reflection. It was approximately 17 nm. Similar XRD result was reported during green synthesis of AuNPs using various plants extracts (Masumeh Noruzia, 2011; Bappi Paul, 2015; Mohanan V. Sujitha, 2013).

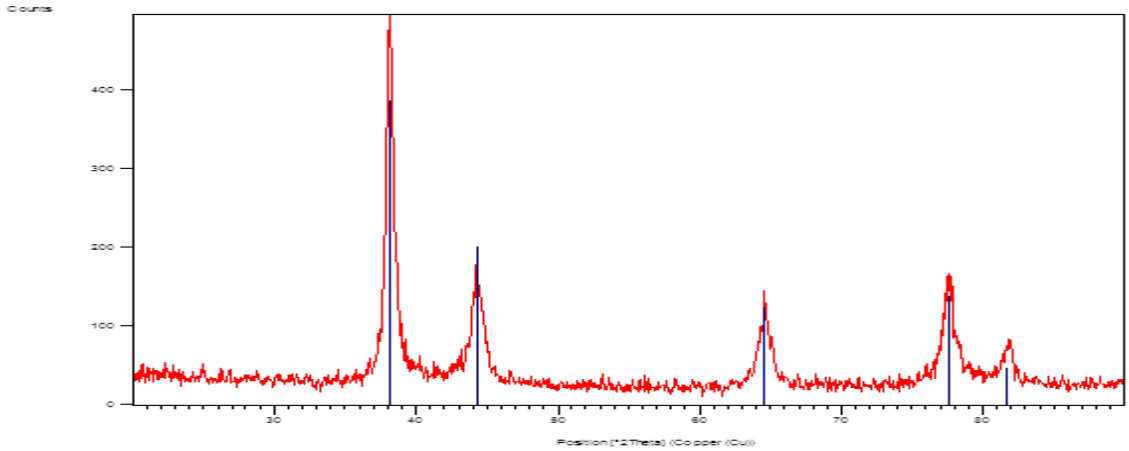

Figure 15: XRD analysis of AuNPs.

The XRD result of the multi-metallic composite particles showed no peaks, which can be due to the fact that the particles were not crystalline (C. Suryanarayana, 1998).

3.6 Transmission electron microscopy (TEM) analysis

3.6.1 AuNPs

As can be seen in figure 16 below, the TEM images of the AuNPs showed there were mainly three different shapes and sizes. The NPs consist of mainly spherical gold nanoparticles (51–70 nm), along with few rods (71–80 nm), triangular (61-70 nm) and pentagonal shaped (61-70 nm). The particles with hexagonal morphology were the largest in size whereas the particles with spherical morphology were the smallest. The size difference between TEM result and Scherrer's equation might be due the fact that

Scherrer's equation determines the size of crystallite. In general the larger size of nanoparticles might be related to higher metal precursor concentration (Amarendra Dhar Dwivedi, 2010; Shashi Prabha Dubeya, 2010). Some of the particles were found in aggregates. The aggregation might be due to excessive Au-(III) ions in the initial solution depleted most of reducing agents and the remained biomolecules were not enough to act as capping and stabilizing agents that could prevent the particles from aggregation (Chun-Gang Yuan, 2017; N. González-Ballesteros, 2017). In addition, it was evidenced that small and a thin layer of materials surrounded the AuNPs, which indicates the possibility of organic-based capping agents inherent in the extract. However, that might not be enough to prevent particles from aggregation (K. Anand, 2015; S. Shiv Shankar, 2004; Mohanan V. Sujitha, 2013).

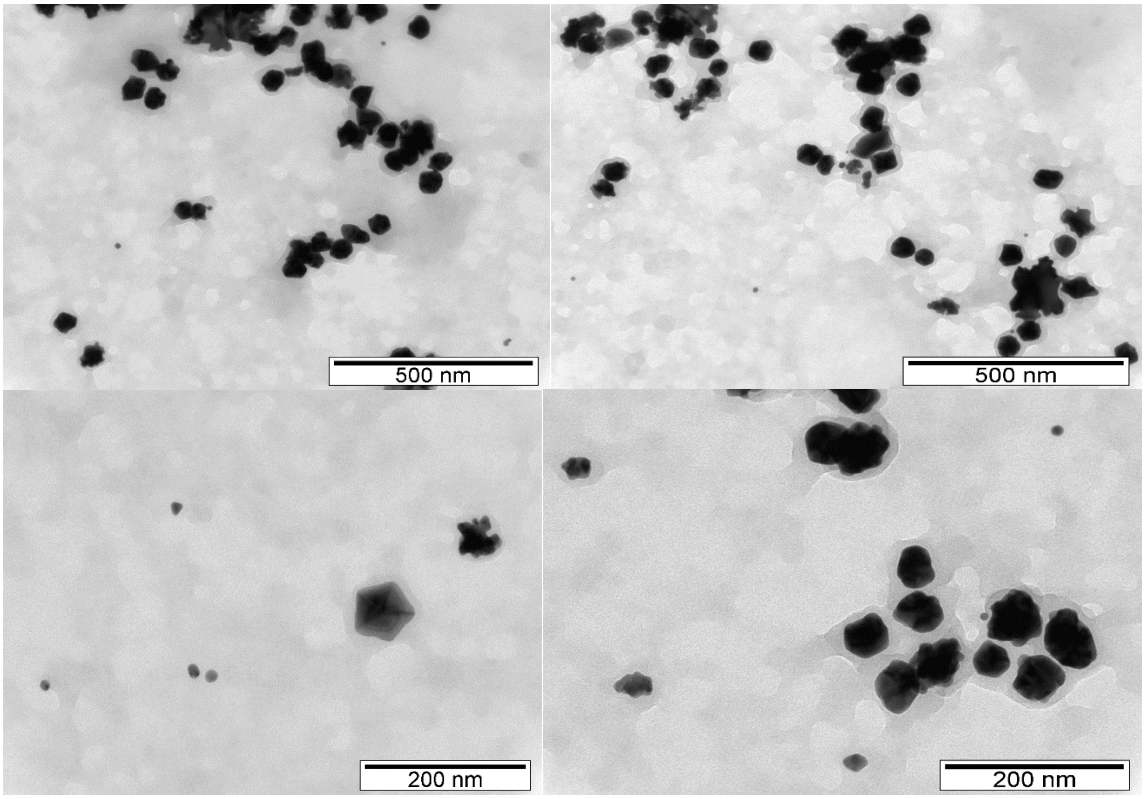

Figure 16 TEM images of AuNPs.

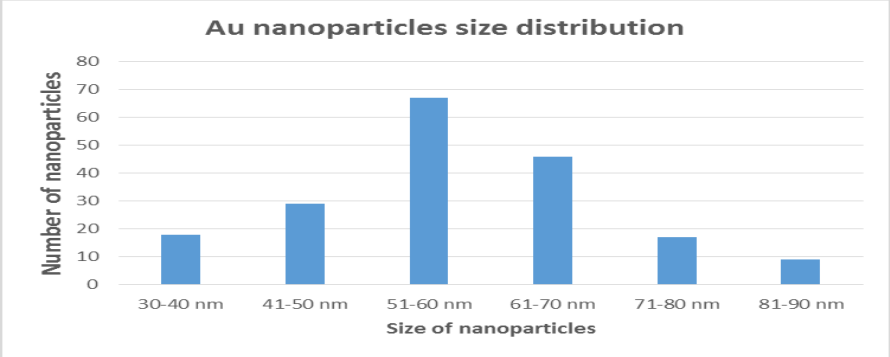

Figure 17: Size distribution of AuNPs.

The electron diffraction (ED) pattern result indicated the crystalline nature of the synthesized AuNPs (Fig. 18 below). It can also be seen from figure 18 that the characteristic ring pattern which added further evidence that the AuNPs were highly crystalline in nature (Kasi Gopinath, 2016). Our result is consistent with previous studies in which AuNPs with different shapes, morphologies and size were obtained using different plant extracts such as onion peel extracts, piper longum fruit, cannonball fruit (Jayachandra Reddy Nakkala, 2016; Jayanta Kumar Patra, 2016; Bappi Paul, 2015; Sathishkumar G., 2016).

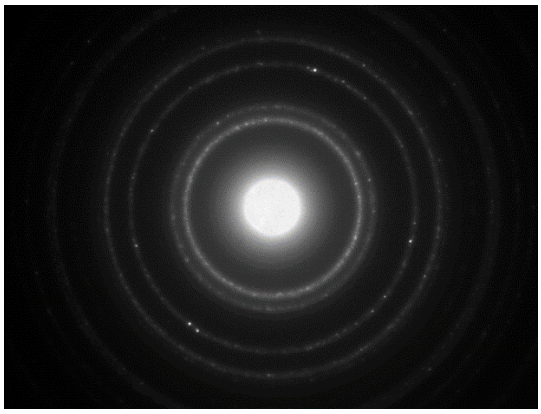

Figure 18 Selected electron diffraction areas of AuNPs.

3.6.2 Multi-metallic nanocomposite particles

As can be seen from the TEM image (figure 19) of multi-metallic composite particle, mostly spherical particles with approximate average size of 100 nm (range between 70-150 nm) were formed. Very few smaller spherical NPs with approximate average size of 40-50 nm formed along with larger irregular shaped particles. Some of the particles formed aggregates and we were unable to measure the exact size. In general the larger NPs size might be related to higher metal precursor concentration (Amarendra

Dhar Dwivedi, 2010; Shashi Prabha Dubeya, 2010). Possible reason for the aggregation could be excessive metal ions (Fe, Al, Zn and Cu) in AMD depleted most of capping and stabilizing agents (Chun-Gang Yuan, 2017; N. González-Ballesteros, 2017).

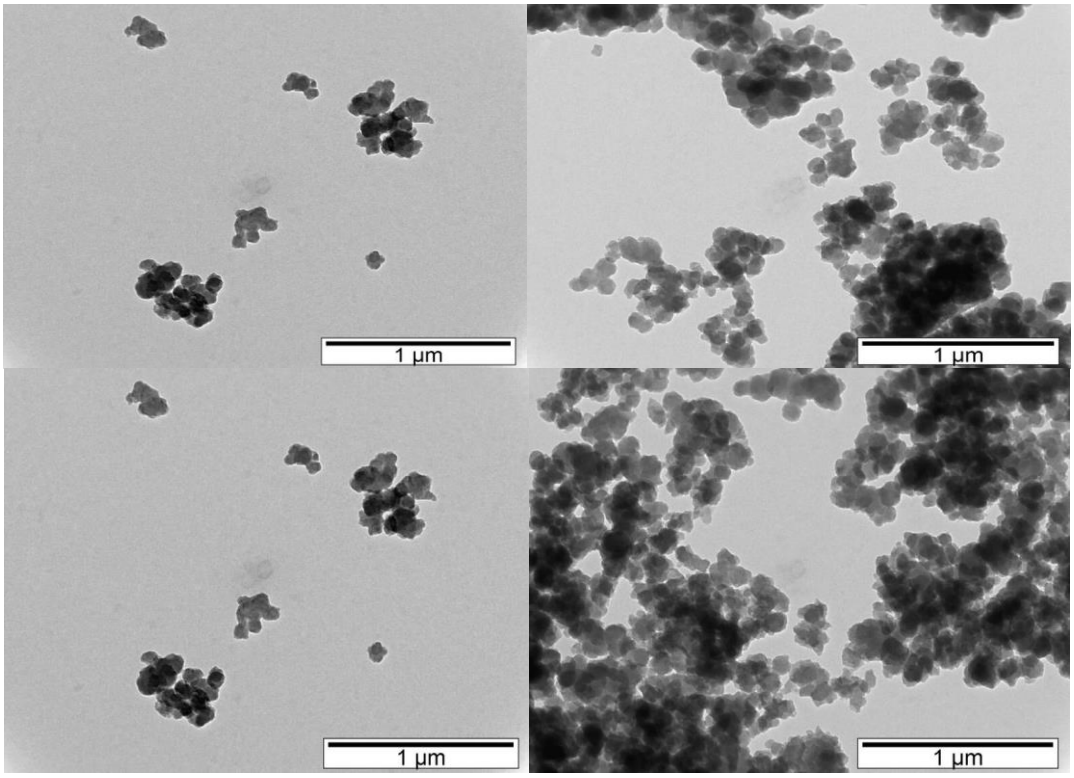

Figure 19: TEM images of multi-metallic composite particles.

The ED result showed (figure 20) the amorphous nature of the multi-metallic composite particles. It showed no ring pattern, which added further evidence that the multi-metallic composite particles were not crystalline in nature (Kasi Gopinath, 2016). The result obtained here was consistent with XRD result obtained, which also indicated the amorphous nature of the particles.

Figure 20: Selected electron diffraction area of multi-metallic composite particles.

3.7 Energy-dispersive X-ray spectroscopy (EDS/EDX) analysis

The synthesized AuNPs were further characterized by EDS analysis, which gave additional evidence for the reduction of Au-(III) solution to Au-(0). The EDS analysis result (Fig. 21 below) confirmed that the only element present in the precipitate was gold. This result was consistent with the XRD analysis outcome. The identification of Cu was due to the composition of the sample grid. The energy peaks for a strong signal were in the range of 2-2.5 keV, 9.5-10 keV and 11-12 keV which match with the earlier observations made by another studies for AuNPs (Pannerselvam Balashanmugama, 2016; Ana Assunçao, 2016; Yao Huang, 2017).

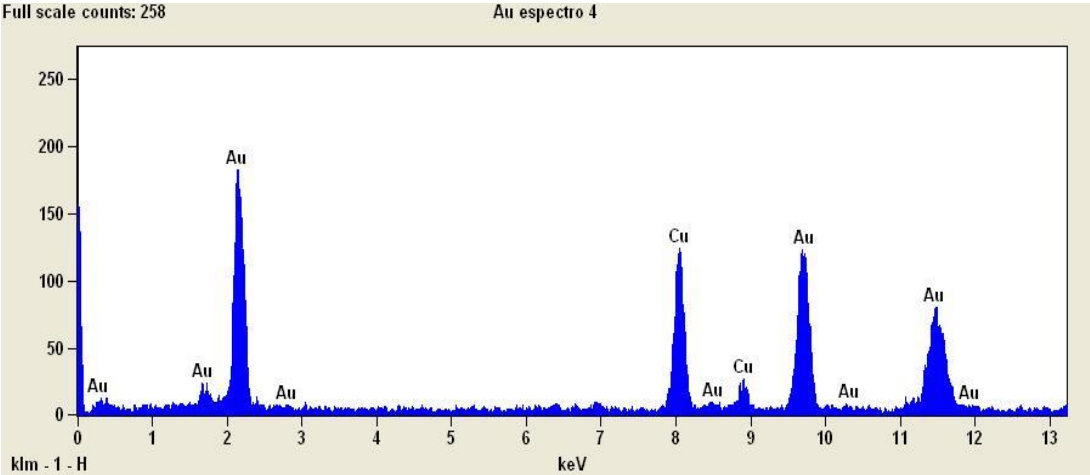

Figure 21 EDS spectroscopy displays the chemical composition of the gold nanoparticles.

The EDS analysis for multi-metallic composite particles (fig. 22 below) revealed that the precipitate mainly contain iron, aluminum, copper. Oxygen was also identified in the precipitate, which may be associated to the metals as metal oxides and/or hydroxide. The identification of Ni was due to the composition of sample grid. The result was in consistent with the wastewater composition analysis done before and after removal of metals from AMD wastewater. The presence of O and C peaks along with the metal signal suggested the multi-metallic composite particles might capped by phyto-constituents through oxygen atom or also this might be related with the presence of the corresponding identified metal oxides (Pannerselvam Balashanmugama, 2016).

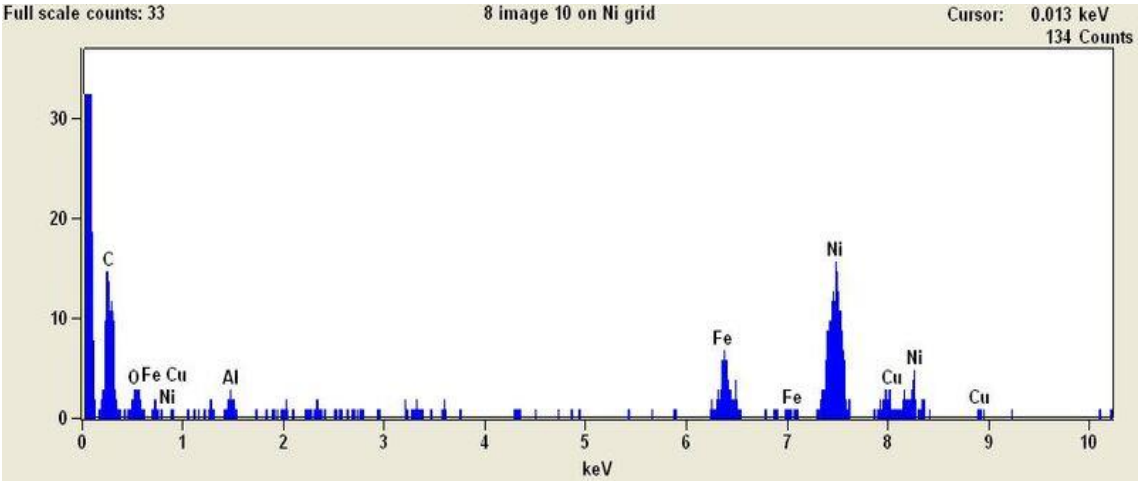

Figure 22 EDS spectroscopy displays the chemical composition of multi-metallic composite particles.

3.8 Zeta Potential analysis

Zeta potential is a key indicator of the stability of colloidal dispersions. The magnitude of the zeta potential indicates the degree of electrostatic repulsion between adjacent, similarly charged particles in dispersion. For molecules and particles that are small enough, a high zeta potential will confer stability, i.e., the solution or dispersion will resist aggregation. When the potential is small, attractive forces may exceed this repulsion and the dispersion may break and flocculate. Therefore, colloids with high zeta potential (negative or positive) are electrically stabilized while colloids with low zeta potentials tend to coagulate or flocculate (Mohanan V. Sujitha, 2013; N. González-Ballesteros, 2017; Pooriya Khademi-Azandehi, 2015). The stability behavior of the colloid is indicated in the table 8 below. According to the information presented here, in our result both AuNPs and multi-metallic composite particles showed moderate to good stability.

Table 8 the stability of colloid particles based on their zeta potential values.

Zeta Potential (mV)	**Stability behavior of the colloid**
0 to (+/-) 5	Rapid Coagulation or flocculation
(+/-) 10 to (+/-) 30	Incipient instability
(+/-) 30 to (+/-) 40	Moderate stability
(+/-) 40 to (+/-) 60	Good stability
More than (+/-) 61	Excellent stability

The zeta potential is caused by the net electrical charge contained within the region bounded by the slipping plane, and also depends on the location of that plane. Thus it is widely used for quantification of the magnitude of the charge. However, zeta potential is not equal to the Stern potential or electric surface potential in the double layer, because these are defined at different locations. Such assumptions of equality should be applied with caution. Nevertheless, zeta potential is often the only available path for characterization of double-layer properties (Pooriya Khademi-Azandehi, 2015).

The stability of AuNPs and multi-metallic composite particles were measured using zeta potentiometer. The zeta potential of the AuNPs is shown in Figure 23 below. The particles showed moderate to good stability at different pH of the solution between pH 3 and 12. The highest stability was showed at pH 7 and 12 whereas the lowest stability at pH 1 and 2. Similar zeta potential values were reported for gold nanoparticles synthesized using *Moringa Oleifera* petals (K. Anand, 2015) and Citrus fruits (Mohanan V. Sujitha, 2013).

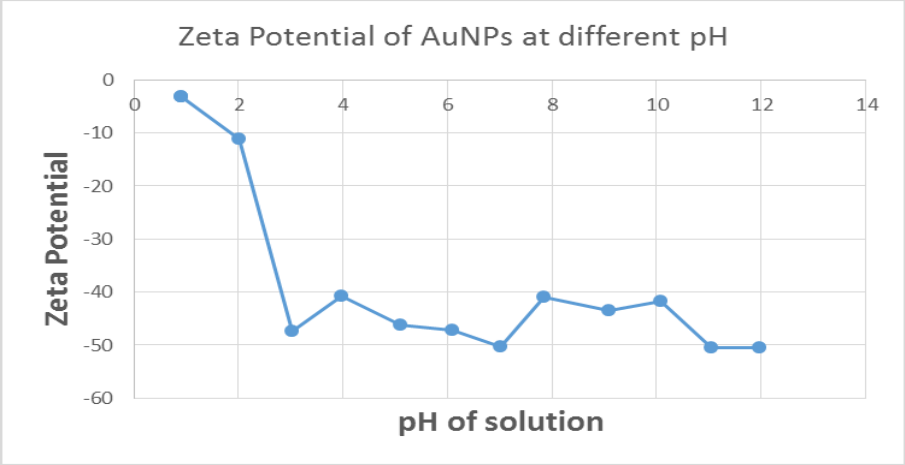

Figure 23 Zeta Potential of AuNPs at different pHs.

As can be seen from Fig. 24 below, the zeta potential of multi-metallic composite particles showed moderate to good stability at pH between 4 and 12 except at pH 8. The zeta potential presented at pH 8 might be the isoelectric point. The moderate to good stability of AuNPs and multi-metallic composite particles might be due to the biomolecules from extract have the ability to bind metal ion and form a coat over the NPs to prevent aggregation (Mohanan V. Sujitha, 2013; N. González-Ballesteros, 2017).

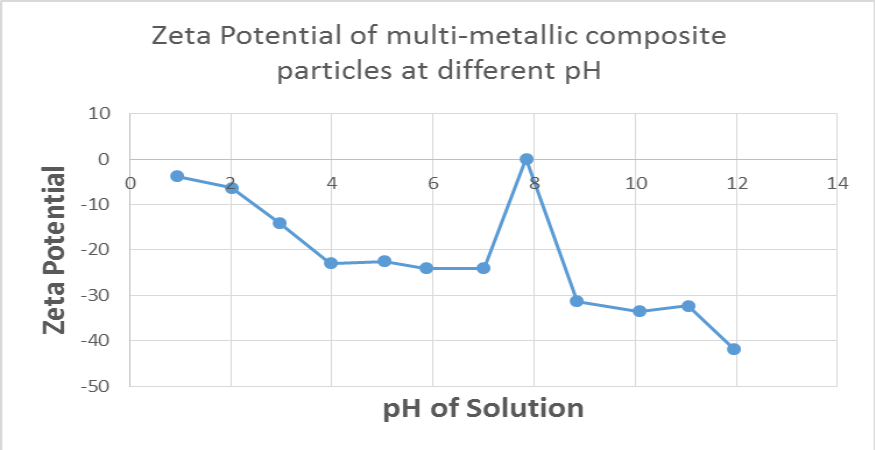

Figure 24 Zeta Potential of multi-metallic composite particles at different pHs.

3.9 Phosphate removal efficiency of multi-metallic composite particles

The pollutant concentration of the synthetic wastewater was measured and showed in the table 9 below. Experiments were carried out to evaluate the performance of synthesized multi-metallic composite particles in treating synthetic wastewater in terms of phosphate removal. The experiments were conducted in batch mode, each cycle running for about 12 hours.

Table 9 Composition of the synthetic wastewater

Composition of synthetic wastewater			
pH	PO_4^{3-}	NO_3^-	COD
7.01 ± 0.05	80 ± 3	30 ± 2	619 ± 24

As can been seen in Fig. 25 and Fig. 26 below, the removal efficiency of phosphate was relatively higher (more than 50 %) for 1 g/L adsorbent in wastewater and more than 35% for 0.5 g/L adsorbent in wastewater ratio during the first 0.5 hour. Generally, it was evidenced that the removal efficiency slightly increases as the time of adsorption increases. Significant ($p<0.05$) amount of phosphate were adsorbed at first 0.5 hour for both adsorbent concentration (1 g/L and 0.5 g/L). Similar rapid adsorption progress was reported in another study (Asya Drenkova-Tuhtan, 2017). Mostly, the removal efficiency of phosphate increased significantly ($P<0.05$) as the time of adsorption increase (up to 6 hours). However, there was no significant ($P=0.12$) increase in the removal efficiency between adsorption time 6 hours and 12 hours for adsorbent concentration of 1 g/L. No significant removal efficiency increase ($P=0.06$) between 6 hours and 12 hours for 0.5 g/L adsorbent concentration as well.

The higher initial adsorption rate at 0.5h of might be related to a lot of free adsorption sites at the very beginning of adsorption process. This might also be favored by the driving force of higher initial

phosphate concentration (Dimitris Mitrogiannis, 2017). In contrast, the slow adsorption rate increment after 0.5hr might be due to the higher initial phosphate concentration that requires more time to achieve equilibrium. No significant increase after 6h might be due all of the active site of the adsorbent were filled with phosphate and the equilibrium was approached (Asya Drenkova-Tuhtan, 2017; Dimitris Mitrogiannis, 2017). Therefore, we have selected 6h of adsorption time as the optimum adsorption time since no significant increment was observed thereafter.

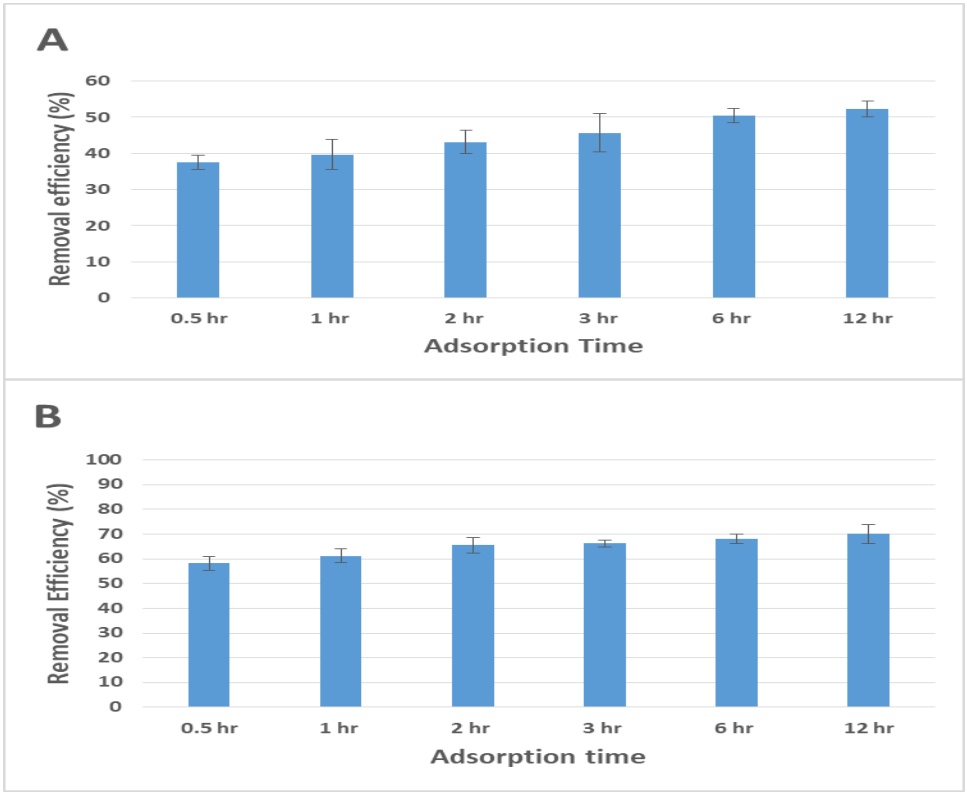

Figure 25: Phosphate removal efficiency of multi-metallic composite particles using adsorbent concentration. (A) 0.5 g/L, (B) 1g/L

In comparison the results from 0.5 g/L and 1 g/L adsorbent concentration, significantly higher ($P<0.05$) removal efficiency were observed by 1 g/L adsorbent concentration. Possible reason for higher removal efficiency of 1 g/L adsorbent concentration could be the presence of more adsorbing sites because of more adsorbent were used (Asya Drenkova-Tuhtan, 2017; Dimitris Mitrogiannis, 2017).

In comparison to other phosphate removal studies via adsorption, such as adsorption using $Ca(OH)_2$ treated natural clinoptilolite (Dimitris Mitrogiannis, 2017), using nanocomposite magnetic particles functionalized with ZnFeZr-adsorbent (Asya Drenkova-Tuhtan, 2017), using nanosized lanthanum hydroxide doped onto magnetic reduced graphene oxide (Hamid Rashidi Nodeh, 2017), using zero valent iron(ZVI) (Nathalie Sleiman, 2017), using Iron oxide nanoparticles (Dan Cao, 2016), competitive

and promising removal efficiency reported in our result with lower adsorbent concentration (g/L) and shorter adsorption time. In comparison of these results to other biological treatment methods such as constructed wetland (Pei Luo, 2017) and activated sludge (Yue Yuan, 2016), the removal efficiency observed by multi-metallic composite particles was much better.

The exact mechanism of phosphate sorption on various adsorbent materials is a subject of ongoing investigation. It is well known that the main mechanisms of reversible phosphate sorption on metals composite particles involve electrostatic attraction to protonated hydroxyl groups, ligand exchange forming a covalent bond with a metallic cation (inner sphere surface complexation), ion exchange against OH^- (outer sphere surface complexation) and hydrogen bonding (Asya Drenkova-Tuhtan, 2017).

4. Conclusion and recommendations

4.1 Conclusion

In this study suitable, rapid, eco-friendly, nontoxic, cost effective, and single pot synthesis methods were developed for the production of AuNPs and multi-metallic composite particles using extract of raspberry waste leaves. This study also revealed the potential utilization of acid mine drainage wastewater as a source of multi-metallic composite particles which was proved to be efficient for the remove of phosphate from wastewaters via adsorption.

The waste raspberry leaf extract acted as a reducing and capping agent for the synthesis of AuNPs from Au-(III) chloride solution. The leave extract was also successful to obtain multi-metallic composite particles from acid mine drainage wastewater. Thus high removal efficiency of Au-(III) and Fe from a synthetic solution and from acid mine drainage was obtained, respectively, using dried raspberry leave extract. The produced AuNPs was confirmed to be pure and crystalline Au-(0) according to different characterization techniques. The characterization study of the multi-metallic composite particles suggested that the particles are mainly composed by iron, aluminum and copper, probably as oxides. The study also suggested the particles are not crystalline.

The synthesized AuNPs and multi-metallic composite particles have moderate to good stability in aqueous solution at different pHs. Most of the AuNPs and multi-metallic composite particles formed were spherical. The synthesized multi-metallic composite particles showed phosphate removal efficiency up to 70.0 ± 3.9 % from synthetic wastewater at optimized conditions.

4.2 Recommendation

- ✓ Exploring various applications of the synthesized gold nanoparticles such as catalysis, anti-cancer and antibacterial activity etc.
- ✓ Optimization of phosphate removal efficiency using different solid/liquid ratios and different pHs and temperature of the solutions etc.
- ✓ Desorption study of phosphate to get optimum cycle of adsorbent usage and possible recovery of phosphate.

Bibliography

A. Jafaripour, N. R. (2015). Utilisation of residue gas sludge (BOS sludge) for removal of heavy metals from acid mine drainage (AMD). *International Journal of Mineral Processing*, 90-96.

A. Rai, A. S. (2006). Role of halide ions and temperature on the morphology of biologically synthesized gold nanotriangles. *Langmuir*, 736-741.

Adam Truskewycza, R. S. (2016). Iron nanoparticles synthesized using green tea extracts for the fenton-like degradation of concentrated dye mixtures at elevated temperatures. *Journal of Environmental Chemical Engineering*, 4409-4417.

Akbar Soliemanzadeh, M. F. (2017). The application of green tea extract to prepare bentonite-supported nanoscale zero-valent iron and its performance on removal of Cr(VI): Effect of relative parameters and soil experiments. *Microporous and Mesoporous Materials*, 60-69.

Akbar Soliemanzadeh, M. F. (2017). The application of green tea extract to prepare bentonite-supported nanoscale zero-valent iron and its performance on removal of Cr(VI): Effect of relative parameters and soil experiments. *Microporous and Mesoporous Materials*, 60-69.

Amarendra Dhar Dwivedi, K. G. (2010). Biosynthesis of silver and gold nanoparticles using Chenopodium album leaf extract. *Colloids and Surfaces A: Physicochemical and Engineering Aspects*, 27-33.

Amit Kumar Mittal, Y. C. (2013). Synthesis of metallic nanoparticles using plant extracts. *Biotechnology Advances*, 346-356.

Ana Assunçao, B. V. (2016). Recovery of gold(0) nanoparticles from aqueous solutions using effluents from a bioremediation process. *The Royal Society of Chemistry*, 112784–112794.

Arthanari Saravanakumar, M. G. (2015). Biosynthesis of silver nanoparticles using Cassia tora leaf extract and its antioxidant and antibacterial activities. *Journal of Industrial and Engineering Chemistry*, 277-281.

Arun Kumar Thalla, S. Y. (2016). Green synthesis of iron nanoparticles using different leaf extracts for treatment of domestic waste water. *Journal of Cleaner Production*, 1425-1435.

Asya Drenkova-Tuhtan, M. S. (2017). Pilot-scale removal and recovery of dissolved phosphate from secondary wastewater effluents with reusable ZnFeZr adsorbent Fe3O4/SiO2 particles with magnetic harvesting. *Water Research*, 77-87.

B. Ajithaa, Y. A. (2016). Sesbania grandiflora leaf extract assisted green synthesis of silver nanoparticles: Antimicrobial activity. *Materials Today*, 1977-1984.

Bappi Paul, B. P. (2015). Greensynthesis of gold nano particles using Pogestemonbenghalensis (B) O. Ktz. leaf extract and studies of their photocatalytic activity in degradation of methylene blue. *Materials Letters*, 37-40.

C. Krishnaraj, E. J. (2010). Synthesis of silver nanoparticles using Acalypha indica leaf extracts and its antibacterial activity against water borne pathogens. *Colloids and Surfaces B: Biointerfaces*, 50-56.

C. Mystrioti, T. X. (2016). Comparative evaluation of five plant extracts and juices for nanoiron synthesis and application for hexavalent chromium reduction. *Science of the Total Environment, 539*, 105-113.

C. Mystrioti, T. X. (2016). Comparative evaluation of five plant extracts and juices for nanoiron synthesis and application for hexavalent chromium reduction. *Science of the Total Environment*, 105-113.

C. Suryanarayana, M. G. (1998). *X-Ray Diffraction A Practical Approach.* New York: Springer Science+Business Media, LLC.

C.K.S. Pillai, W. P. (2009). Chitin and chitosan polymers: Chemistry, solubility and fiber formation. *Progress in Polymer Science*, 641-678.

C.P. Devatha, A. K. (2016). Green synthesis of iron nanoparticles using different leaf extracts for treatment of domestic waste water. *Journal of Cleaner Production*, 1425-1435.

Chun-Gang Yuan, C. H. (2017). Biosynthesis ofgold nanoparticles using Capsicum annuum var. grossum pulp extract and its catalytic activity. *Physica E*, 19-26.

D. Barrie Johnson, K. B. (2005). Acid mine drainage remediation options: a review. *Science of the Total Environment*, 2-14.

Dan Cao, X. J. (2016). Removal of phosphate using iron oxide nanoparticles synthesized by eucalyptus leaf extract in the presence of CTAB surfactant. *Chemosphere*, 23-31.

Dimitris Mitrogiannis, M. P. (2017). Removal of phosphate from aqueous solutions by adsorption onto Ca(OH)2 treated natural clinoptilolite. *Chemical Engineering Journal*, 510-522.

E.Y. Seo, Y. C. (2017). Recovery of Fe, Al and Mn in acid coal mine drainage by sequential selective precipitation with control of pH. *Catena*, 11-16.

Egerton, R. F. (2005). *Physical Principles of Electron Microscopy .* Alberta: Springer .

Eppler AS, R. G. (2000). Thermal and chemical stability and adhesion strength of Pt nanoparticle arrays supported on silica studied by transmission electron microscopy and atomic force microscopy. *Journal of Physical Chemistry* , 7286-7292.

Evgenia Iakovleva, E. M. (2015). Acid mine drainage (AMD) treatment: Neutralization and toxic elements removal with unmodified and modified limestone. *Ecological Engineering*, 30-40.

H. Joy Prabu, I. J. (2015). Plant-mediated biosynthesis and characterization of silver nanoparticles by leaf extracts of Tragia involucrata, Cymbopogon citronella, Solanum verbascifolium and Tylophora ovata. *Karbala International Journal of Modern Science*, 237-246.

Hamid Rashidi Nodeh, H. S. (2017). Enhanced removal of phosphate and nitrate ions from aqueous media using nanosized lanthanum hydrous doped on magnetic graphene nanocomposite. *Journal of Environmental Management*, 265-274.

Hossain M. Azam, K. T. (2014). Fe(III) reduction-mediated phosphate removal as vivianite . *Chemosphere*, 1-9.

Iris F. F. Benzie, J. J. (1996). The Ferric Reducing Ability of Plasma (FRAP) as a Measure of ‘‘Antioxidant Power’’: The FRAP Assay. *ANALYTICAL BIOCHEMISTRY*, 70-76.

J. Das, M. P. (2013). Sesbania grandiflora leaf extract mediated green synthesis of antibacterial silver nanoparticles against selected human pathogens. *Spectrochimica Acta Part A: Molecular and Biomolecular Spectroscopy*, 265-70.

Jasmine Jacob, T. M. (2012). A simple approach for facile synthesis of Ag, anisotropic Au and bimetallic (Ag/Au). *Materials Science and Engineering C*, 1827-1834.

Jayachandra Reddy Nakkala, R. M. (2016). The antioxidant and catalytic activities of green synthesized gold nanoparticles from Piper longum fruit extract. *Process Safety and Environmental Protection*, 288-294.

Jayanta Kumar Patra, Y. K.-H. (2016). Green biosynthesis of gold nanoparticles by onion peel extract: Synthesis, characterization and biological activities. *Advanced Powder Technology*, 2204-2213.

Jia Yu, D. H. (2016). Facile one-step green synthesis of gold nanoparticles using Citrus maxima aqueous extracts and its catalytic activity. *Materials Letters*, 110-112.

Jing Liu, L. Z.-E. (2017). Enhancing As(V) adsorption and passivation using biologically formed nano-sized FeS coatings on limestone: Implications for acid mine drainage treatment and neutralization. *Chemosphere*, 529-538.

K. Anand, R. G. (2015). Agroforestry waste Moringa oleifera petals mediated green synthesis of gold nanoparticles and their anti-cancer and catalytic activity. *Journal of Industrial and Engineering Chemistry*, 1105-1111.

K. Vijayaraghavan a, R. B. (2015). Is biosorption suitable for decontamination of metal-bearing wastewaters? A critical review on the state-of-the-art of biosorption processes and future directions. *Journal of Environmental Management*, 283-296.

K.D. Lee, P. N. (2015). Eco-friendly synthesis of gold nanoparticles (AuNPs) using Inonotus obliquus and their antibacterial, antioxidant and cytotoxic activities. *Journal of Industrial and Engineering Chemistry*, 67-72.

Kasi Gopinath, S. K. (2016). Green synthesis of silver, gold and silver/gold bimetallic nanoparticles using the Gloriosa superba leaf extract and their antibacterial and antibiofilm activities. *Microbial Pathogenesis*, 1-11.

Khan Behlol Ayaz, A. S. (2014). Preparation of gold nanoparticles using Salicornia brachiata plant extract and evaluation of catalytic and antibacterial activity. *Spectrochimica Acta Part A: Molecular and Biomolecular Spectroscopy*, 54-58.

Khwaja Salahuddin Siddiqi, A. H. (2017). Recent advances in plant-mediated engineered gold nanoparticles and their application in biological system. *Journal of Trace Elements in Medicine and Biology*, 10-23.

Lanlan Huang, X. W. (2014). Green synthesis of iron nanoparticles by various tea extracts: Comparative study of the reactivity. *Biomolecular Spectroscopy*, 295-301.

M. Kobya, E. D. (2017). Treatments of alkaline non-cyanide, alkaline cyanide and acidic zinc electroplating wastewaters by electrocoagulation. *Process Safety and Environmental Protection*, 373-385.

M. Sigamoney, S. S. (2016). African leafy vegetables as bio-factories for silver nanoparticles: A case study on Amaranthus dubius C Mart. Ex Thell. *South African Journal of Botany*, 230-240.

M.A. Martín-Lara, G. B. (2014). New treatment of real electroplating wastewater containing heavy metal ions by adsorption onto olive stone. *Journal of Cleaner Production*, 120-129.

María Martínez-Cabanas, M. L.-G. (2016). Green synthesis of iron oxide nanoparticles. Development of magnetic hybrid materials for efficient As(V) removal. *Chemical Engineering Journal*, 83-91.

Masumeh Noruzia, D. Z. (2011). Rapid green synthesis of gold nanoparticles using Rosa hybrida petal extract at room temperature. *Spectrochimica Acta Part A: Molecular and Biomolecular Spectroscopy*, 1461-1465.

Michael Iv, N. T.-L. (2015). Clinical applications of iron oxide nanoparticles for magnetic resonance imaging of brain tumors. *Nonomedicine*, 993-1018.

Minseok Kim, K. P. (2016). Phosphate recovery from livestock wastewater using iron oxide nanotubes . *Chemical Engineering Research and Design*, 119-128.

Mohammad A. Khalilzadeh, M. B. (2016). Green synthesis of silver nanoparticles using onion extract and their application for the preparation of a modified electrode for determination of ascorbic acid. *Journal of Food and Drug Analysis* , 796-803.

Mohanan V. Sujitha, S. K. (2013). Green synthesis of gold nanoparticles using Citrus fruits (Citrus limon, Citrus reticulata and Citrus sinensis) aqueous extract and its characterization. *Spectrochimica Acta Part A: Molecular and Biomolecular Spectroscopy*, 12-23.

Mohit Chaudhary, P. B. (2016). Synthesis of iron oxyhydroxide nanoparticles and its application for fluoride removal from water. *Journal of Environmental Chemical Engineering*, 4897-4903.

Moo Joon Shim, B. Y.-S. (2015). Water quality changes in acid mine drainage streams in Gangneung,Korea, 10 years after treatment with limestone. *Journal of Geochemical Exploration*, 234-242.

Muhammad Jamil Ahmed, G. A. (2015). Green synthesis of silver nanoparticles using leaves extract of Skimmia laureola: Characterization and antibacterial activity. *MaterialsLetters*, 10-13.

N. González-Ballesteros, S. P.-L.-G.-A. (2017). Green synthesis of gold nanoparticles using brown algae Cystoseirabaccata: Its activity in colon cancer cells. *Colloids and Surfaces B: Biointerfaces*, 90-98.

Nabeel Ahmad, S. B. (2017). Biosynthesis and characterization of gold nanoparticles: Kinetics, in vitro and in vivo study. *Materials Science and Engineering C*, 553-564.

Nathalie Sleiman, V. D.-N. (2017). Phosphate removal from aqueous solutions using zero valent iron(ZVI): Influence of solution composition and ZVI aging. *Colloids and Surfaces A: Physicochemical and Engineering Aspects*, 1-10.

Niederberger, F. J. (2013). The fascinating world of nanoparticle. *Materials Today*, 262-271.

Olivier Lefebvrea, C. M. (2012). Bioelectrochemical treatment of acid mine drainage dominated with iron . *Journal of Hazardous Materials*, 411-417.

P. Mohanpuria, N. R. (2008). Biosynthesis of nanoparticles: technological concepts and future applications. *Journal Nanopart*, 507-517.

P.P.N. Vijay Kumara, S. P. (2014). Green synthesis and characterization of silver nanoparticles using Boerhaavia diffusa plant extract and their anti bacterial activity. *Industrial Crops and Products*, 562-566.

Palaniselvam Kuppusamy, M. M. (2016). Biosynthesis of metallic nanoparticles using plant derivatives and their new avenues in pharmacological applications – An updated report. *Saudi Pharmaceutical Journal*, 473-484.

Palaniselvam Kuppusamy, M. M. (2016). Biosynthesis of metallic nanoparticles using plant derivatives and their new avenues in pharmacological applications – An updated report. *Saudi Pharmaceutical Journal*, 473-484.

Palaniselvam Kuppusamy, S. J. (2015). Intracellular biosynthesis of Au and Ag nanoparticles using ethanolic extract of Brassica oleracea physicochemical and biological properties L. and studies on their physicochemical and biological properties. *Journal of Environmental Science*, 151-157.

Pannerselvam Balashanmugama, P. D. (2016). Phytosynthesized gold nanoparticles fromC. roxburghii DC. leaf and their toxic effects on normal and cancer cell lines. *Journal of Photochemistry & Photobiology, B: Biology*, 163-173.

Pei Luo, F. L. (2017). Phosphorus removal from lagoon-pretreated swine wastewater by pilot-scale surface flow constructed wetlands planted with Myriophyllum aquaticum. *Science of the Total Environment*, 490-497.

Peter Logeswari, S. S. (2015). Synthesis of silver nanoparticles using plants extract and analysis of their antimicrobial property. *Journal of Saudi Chemical Society*, 311-217.

Pooriya Khademi-Azandehi, J. M. (2015). Green synthesis, characterization and physiological stability of goldnanoparticles from Stachys lavandulifolia Vahl extract. *Particuology*, 22-26.

Prakash, N. S. (2011). Factors affecting the geometry of silver nanoparticles synthesis in Chrysosporium tropicum and Fusarium oxusporum. *American Journal of Nanotechnology*, 112-121.

Priyanka Singh, Y.-J. K.-C. (2016). Biological Synthesis of Nanoparticles from Plants and Microorganisms. *Trends in Biotechnology*, 588-599.

Raju, D. M. (2011). Synthesis of gold nanoparticles by various leaf fractions of Semecarpus anacardium L. . *Trees*, 145-151.

Rani Mata, A. B. (2016). Green-synthesized gold nanoparticles from Plumeria alba flowerextract to augment catalytic degradation of organic dyes and inhibitbacterial growth. *Particuology*, 78-86.

S. Machado, W. S. (2013). Application of green zero-valent iron nanoparticles to the remediation of soils contaminated with ibuprofen. *Science of the Total Environment*, 323-329.

S. Shiv Shankar, A. R. (2004). Rapid synthesis of Au, Ag, and bimetallic Au core–Ag shell nanoparticles using Neem (Azadirachta indica) leaf broth. *Journal of Colloid and Interface Science*, 496-502.

S. V. N. T. Kuchibhatla, A. S. (2012). Influence of aging and environment on nanoparticle chemistry: implication to confinement effects in nanoceria . *Journal of Physical Chemistry* , 7001-7010.

S.S. Godipurgea, S. Y. (2016). A facile and green strategy for the synthesis of Au, Ag and Au–Ag alloy nanoparticles using aerial parts of R. hypocrateriformis extract and their biological evaluation . *Enzyme and Microbial Technology*, 174-184.

S.S. Godipurgea, S. Y. (2016). A facile and green strategy for the synthesis of Au, Ag and Au–Ag alloynanoparticles using aerial parts of R. hypocrateriformis extract and their biological evaluation. *Enzyme and Microbial Technology*, 174-184.

Sathishkumar G., P. K. (2016). Cannonball fruit (Couroupita guianensis, Aubl.) extract mediated synthesis of gold nanoparticles and evaluation of its antioxidant activity. *Journal of Molecular Liquids*, 229-236.

Sathishkumar, P. K. (2016). Cannonball fruit (Couroupita guianensis, Aubl.) extract mediated synthesis of gold nanoparticles and evaluation of its antioxidant activity. *Journal of Molecular Liquids*, 229-236.

Shakeel Ahmed, M. A. (2016). A review on plants extract mediated synthesis of silver nanoparticles for antimicrobial applications: A green expertise. *Journal of Advanced Research*, 17-25.

Shankar S.S., A. A. (2003). Geranium leaf assisted biosynthesis of silver nanoparticles. *Biotechnology Process*, 1627-1631.

Shashi Prabha Dubeya, M. L. (2010). Green synthesis and characterizations of silver and gold nanoparticles using leaf extract of Rosa rugosa. *Colloids and Surfaces A: Physicochemical and Engineering Aspects*, 34-41.

Silvia Groiss, R. S. (2017). Structural characterization, antibacterial and catalytic effect of iron oxide nanoparticles synthesised using the leaf extract of Cynometra ramiflora. *Journal of Molecular Structure*, 572-578.

Sovan Lal Pal, U. J. (2011). Nanoparticle: An overview of preparation and characterization. *Journal of Applied Pharmaceutical Science*, 228-234.

Ting Wang, J. L. (2014). Green synthesized iron nanoparticles by green tea and eucalyptus leaves extracts used for removal of nitrate in aqueous solution. *Journal of Cleaner Production*, 413-419.

Utkarsha Shedbalkar, R. S. (2014). Microbial synthesis of gold nanoparticles: Current status and future prospects. *Advances in Colloid and Interface Science*, 40-48.

V. Armendariz, I. H.-V. (2004). Size controlled gold nanoparticle formation by Avena sativa biomass: use of plants in nanobiotechnology. *Journal of Nanoparticle Research*, 377-382.

V. Sarathy, P. G. (2008). Aging of iron nanoparticles in aqueous solution: effects on structure and reactivity . *The Journal of Physical Chemistry*, 2286-2293.

W.M. Salema, M. W. (2014). Antibacterial activityofsilvernanoparticlessynthesizedfromlatex and leafextractof Ficus sycomorus. *Industrial Cropsand Products*, 228-234.

Xiaolei Qu, P. J. (2013). Applications of nanotechnology in water and wastewater treatment. *water r e s e arch*, 3931-3946.

Xiaolei Zhang, S. Y. (2011). Synthesis of nanoparticles by microorganisms and their application in enhancing microbiological reaction rates. *Chemosphere*, 489-494.

Yaneth Vasquez, M. C. (2016). Biochemical passive reactors for treatment of acid mine drainage: Effect of hydraulic retention time on changes in efficiency composition of reactive mixture, and microbial activity. *Chemosphere*, 244-253.

Yao Huang, Y. F. (2017). One-step synthesis of size-tunable gold nanoparticles immobilized on chitin nanofibrils via green pathway and their potential applications. *Chemical Engineering Journal*, 573-582.

Young-Soo Han, S.-J. Y.-C. (2017). Geochemical and eco-toxicological characteristics of streamwater and its sediments affected by acid mine drainage. *Catena*, 52-59.

Yue Yuan, J. L. (2016). Improving municipal wastewater nitrogen and phosphorous removal by feeding sludge fermentation products to sequencing batch reactor (SBR). *Bioresource Technology*, 326-334.

APPENDIX

1. **Calibration graph for FRAP experiment**

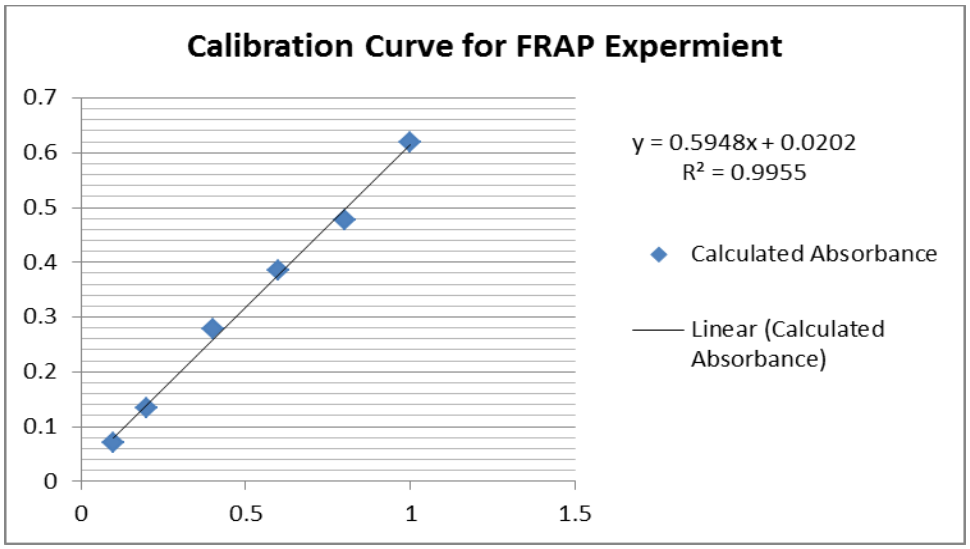

2. **Calibration graph for alumuinum anaylsis**

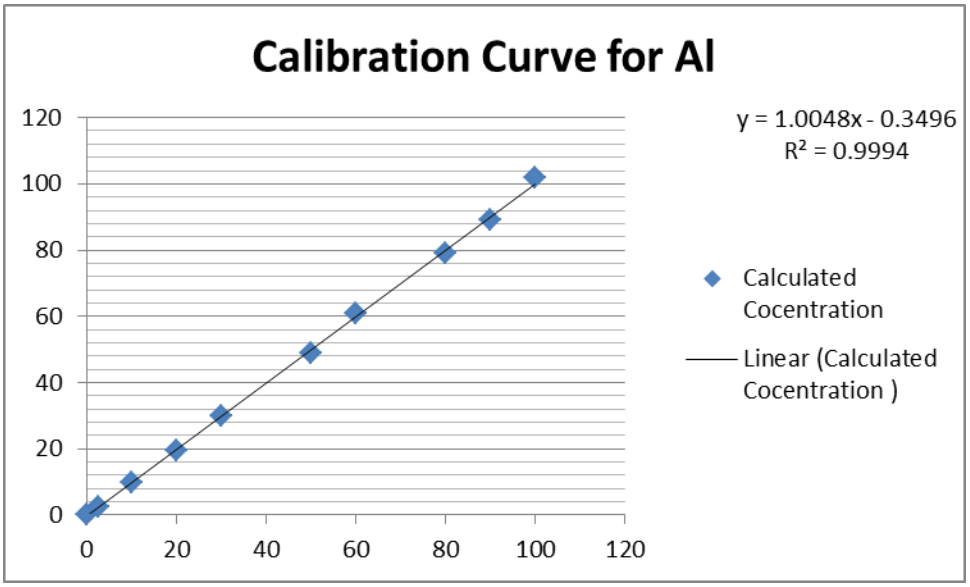

3. **Calibration graph for zinc analysis**

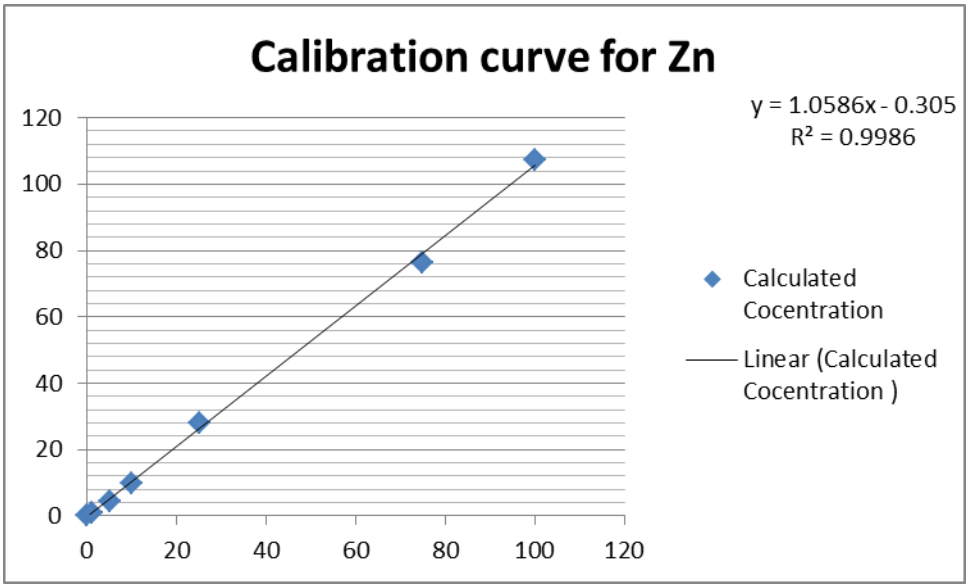

4. **Calibration curve for copper analysis**

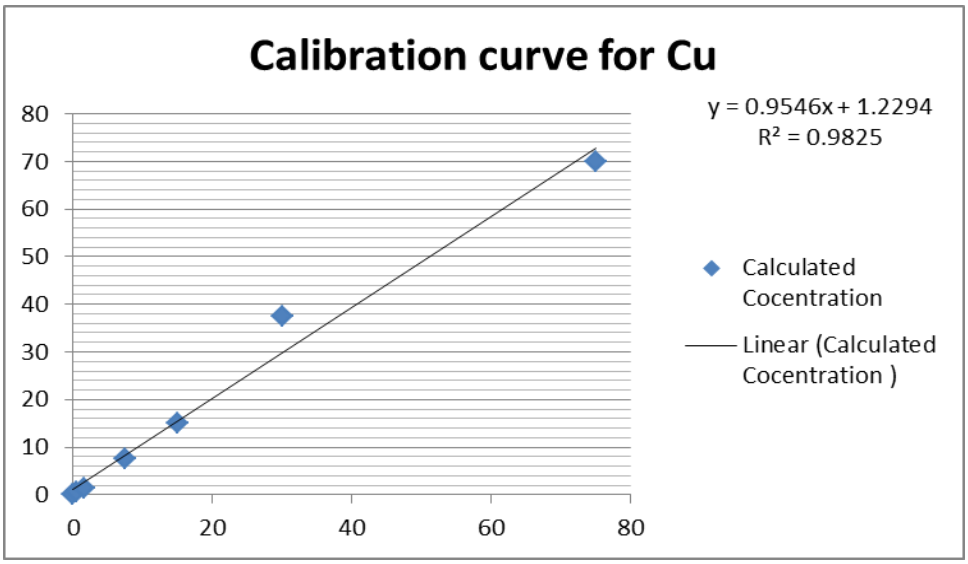

5. Calibration curve for iron analysis